AD_____

Award Number: DAMD17-02-1-0313

TITLE: Structural Basis for Bcl-2-Regulated Mitochondrion-Dependent Apoptosis

PRINCIPAL INVESTIGATOR: Francesca M. Marassi, Ph.D.

CONTRACTING ORGANIZATION: The Burnham Institute
La Jolla, California 92037

REPORT DATE: April 2004

TYPE OF REPORT: Annual

PREPARED FOR: U.S. Army Medical Research and Materiel Command
Fort Detrick, Maryland 21702-5012

REPORT DOCUMENTATION PAGE

Form Approved
OMB No. 074-0188

1. AGENCY USE ONLY (Leave blank)	2. REPORT DATE	3. REPORT TYPE AND DATES COVERED
	April 2004	Annual (15 Mar 03-14 Mar 04)

4. TITLE AND SUBTITLE
Structural Basis for Bcl-2-Regulated Mitochondrion-Dependent Apoptosis

5. FUNDING NUMBERS
DAMD17-02-1-0313

6. AUTHOR(S)
Francesca M. Marassi, Ph.D.

7. PERFORMING ORGANIZATION NAME(S) AND ADDRESS(ES)
The Burnham Institute
La Jolla, California 92037

E-Mail: fmarassi@burnham.org

8. PERFORMING ORGANIZATION REPORT NUMBER

9. SPONSORING / MONITORING AGENCY NAME(S) AND ADDRESS(ES)
U.S. Army Medical Research and Materiel Command
Fort Detrick, Maryland 21702-5012

10. SPONSORING / MONITORING AGENCY REPORT NUMBER

11. SUPPLEMENTARY NOTES

12a. DISTRIBUTION / AVAILABILITY STATEMENT
Approved for Public Release; Distribution Unlimited

12b. DISTRIBUTION CODE

13. ABSTRACT (Maximum 200 Words)

The Bcl-2 family proteins are key regulators of programmed cell death, in health and major human diseases, including cancer. Their pro- or anti-apoptotic functions are regulated by subcellular location, as the proteins cycle between soluble and membrane-bound forms; by dimerization with other Bcl-2 family members; by binding to other non-homologous proteins; and by formation of membrane pores that are believed to regulate apoptosis by perturbing mitochondrial physiology. The solution structures of several Bcl-2 family proteins are very similar despite their antagonistic activities, however, the structures of the membrane-associated proteins are not known and may be key to their opposing functions. The goals of this project are: (1) to determine the structures of the membrane-associated Bcl-2 proteins; and (2) to determine their mechanism of apoptosis regulation. The research strategy combines NMR structure determination in lipid environments with biological assays carried out in parallel with structure determination.

14. SUBJECT TERMS
Structural Biology; NMR; Bcl-2, Cancer Biology; Ion Channels

15. NUMBER OF PAGES
24

16. PRICE CODE

17. SECURITY CLASSIFICATION OF REPORT	18. SECURITY CLASSIFICATION OF THIS PAGE	19. SECURITY CLASSIFICATION OF ABSTRACT	20. LIMITATION OF ABSTRACT
Unclassified	Unclassified	Unclassified	Unlimited

TABLE OF CONTENTS

INTRODUCTION

The goal of this project is to determine the structures of the membrane-associated Bcl-2 family proteins which play major regulatory roles in programmed cell death or apoptosis. The Bcl-2 family includes both pro- and anti-apoptotic members that exert their activities through dimerization with other Bcl-2 family members, binding to non-homologous proteins, and the formation of ion channels or pores, believed to regulate apoptosis by perturbing mitochondrial physiology. Bcl-2 function is also regulated by subcellular location as the proteins cycle between soluble and membrane-bound forms. The solution structures of several Bcl-2 family proteins are very similar despite their antagonistic activities, however, the structures of the membrane-associated proteins are not known and may be key to their opposing functions. Moreover, most of the structural and functional studies focused on soluble truncated proteins, lacking the C-terminal 20-residue hydrophobic domain, which is present in many of the family members and is important for membrane targeting. We are determining the structures of membrane-bound and full-length Bcl-2 proteins to gain insights to their role in apoptosis. Functional studies are carried out in parallel with structure determination. The results from these studies serve as a platform for additional structural and biological experiments aimed at examining the structural consequences of modifications (mutations, cleavage, phosphorylation, myristoylation) and interactions (with other Bcl-2 and non-homologous proteins), as we attempt to further understand the mechanism of apoptosis regulation by Bcl-2 family proteins. We are focusing our studies on Bcl-xL and Bid, two members of the Bcl-2 family with opposing apoptotic activities. The two proteins share homology only in the BH3 domain, and Bid does not have a hydrophobic C domain.

BODY

The research accomplishments associated with the tasks outlined in the original Statement of Work (SOW) are described below, and, in greater detail, in two manuscripts attached to the report [1, 2].

Specific Aim 1. Determine the structures of the membrane-associated Bcl2 proteins.

(1) Prepare milligrams of isotopically labeled full-length Bcl2 by expression in *E. coli*. We have expressed and purified several recombinant members of the Bcl-2 family, Bcl-xL, Bid, Bim and several of their mutants and truncated forms. The proteins are expressed in *E coli* as His-tagged proteins, or His-tagged TrpΔLE fusion proteins using pET vectors, or as GST fusion proteins using pGEX vectors [1, 2]. Protein expression is obtained in the minimal M9 media used for isotopic labeling, which is required for NMR.

(2) Prepare samples of Bcl2 in lipid bilayers for solid-state NMR, and lipid micelles for solution NMR. We have prepared samples of Bcl-X_L, Bid, and tBid in lipid micelles and lipid bilayers for both solution and solid-state NMR structural studies. Recently, we described new methods for NMR sample preparation and for rapid structure determination of membrane proteins in oriented lipid bilayers [3-5], which are being applied to Bcl-2 proteins. These works are not directly associated with the tasks outlined in the SOW, however one of them [4] acknowledges the grant, because the ideas partially resulted from our experiments on Bcl-2 family proteins, funded by this grant. This manuscript has been included in the appendix (reprint number 3).

(3) Perform NMR experiments on Bcl2 proteins in lipid bilayers. We have obtained NMR spectra of Bcl-X_L, Bid, and tBid, in both lipid micelle and lipid bilayer environments [1, 2]. These spectra provide the first view of their conformations at membranes, and are being analyzed for structure determination. The $^{1}H/^{15}N$ HSQC (heteronuclear single quantum correlation) NMR spectra from the purified proteins are well resolved with the appropriate number of backbone and side chain resonances, reflecting pure and homogenous preparations [1, 2], and we have assigned 80% of the resonances in full-length Bcl-X_L in micelles [unpublished]. These spectra provide the basis for structure-activity-relationship studies with molecules that target Bcl-2 proteins. John Reed, our collaborator on this grant (5% effort), has identified a peptide that binds Bax and Bid and modulates their activities [6], and we are carrying out solution NMR studies to map the binding site on Bid.

(4) Determine the structures using orientation constraints. We have measure several $^{1}H/^{15}N$ orientation restraints from samples of Bid, and of C-terminal-deleted and full-length Bcl-X_L in samples of micelles oriented in stressed polyacrylamide gels, and lipid bilayers oriented on glass slides. We are using these restraints to determine the membrane bound structures. Our studies on Bid and tBid, its activated product of caspase-8 cleavage, demonstrate that tBid associates with the membrane with its helices parallel to the membrane surface but without trans-membrane helix insertion. Thus the cytotoxic activity of tBid at mitochondria may be similar to that observed for antibiotic polypeptides, which bind to the surface of bacterial membranes as amphipathic helices and destabilize the bilayer structure promoting the leakage of cell contents [1].

Specific Aim 2.

The functional studies, carried out in parallel with the structural work, serve the two purposes of (1) testing the functionality of the Bcl-2 samples that we prepare for structure determination, and (2) characterizing the biological functions of wild-type and mutant forms. We have tested the ability of recombinant tBid to induce the release of mitochondrial proteins by incubating it with mitochondria isolated from HeLa cells, assaying the supernatant and pelleted fractions with antibodies to cytochrome-c and SMAC. We also tested the ability of recombinant tBid to bind Bcl-X_L, since this interaction requires the BH3 domain and recombinant tBid contains the mutation M97L in this segment. Recombinant tBid, used in the structural studies, is fully active in its ability to induce cytochrome-c and SMAC release from isolated mitochondria, and its capacity to bind anti-apoptotic Bcl-X_L through its BH3 domain is not disrupted by the M97L mutation. [1].

KEY RESEARCH ACCOMPLISHMENTS

1. We have expressed and purified milligram quantities of Bcl-2 family proteins (full-length Bcl-X_L, tBid, and Bim) that have been notoriously difficult to express and purify because of either poor solubility (Bcl-X_L) or toxicity (tBid) [1].
2. We have determined the secondary structure and topology of Bcl-X_L and tBid in membrane environments [1, 2].
3. We have confirmed the biological activity of recombinant tBid produced for NMR studies in bilayers [1].
4. We have assigned 80% of the spectrum of full-length Bcl-X_L, including its hydrophobic C-terminus, in lipid micelles, and have obtained orientation restraints for structure determination [unpublished].

REPORTABLE OUTCOMES

Publications directly related to the tasks associated with the SOW of DAMD17-02-1-0313.

Franzin C.M., Choi J., Zhai D., Reed J.C., and Marassi F.M. (2004). **Structural studies of apoptosis and ion transport regulatory proteins in membranes**. *Magn. Reson. Chem.* 42, 172-179.

Gong X.-M., Choi J., Franzin C.M., Zhai D., Reed J.C., and Marassi F.M. (2004). **Conformation of membrane-associated pro-apoptotic tBid**. *J. Biol. Chem.* 279, 28954-28960.

Publications that acknowledge support of DAMD17-02-1-0313.

Marassi, F.M., and Opella, S.J. (2003). **Simultaneous assignment and structure determination of a membrane protein from NMR orientational restraints**. *Protein Sci. 12*, 403-411.

Invited Presentations that acknowledged support of DAMD17-02-1-0313.

Marassi F.M. (2003). **Imaging membrane proteins in lipid bilayers with NMR**. PENCE Structural Biology Seminar Series, Department of Biochemistry, University of Alberta, Edmonton, Canada.

Marassi F.M. (2004). **NMR Structural studies of apoptosis and ion transport regulatory proteins in membranes.** 5th Biennial Structural Biology Symposium, Tallahasse FL.

Marassi F.M. (2004). **NMR Structural Studies of Proteins in Lipid Bilayers.** Gordon Conference: Chemistry and Biology of Peptides, Ventura CA.

Abstracts that acknowledge support of DAMD17-02-1-0313.

Marassi F.M., Crowell K.J., Franzin C.M., Koltay A., and Reed J. (2003). **NMR of FXYD and Bcl2 family proteins in lipid bilayers and micelles**. Keystone Symposium: Membrane Protein Structure and Mechanism, Poster 416, Taos, NM.

Choi J., and Marassi F.M. (2003). **Structural Studies of the Bcl2 Family Proteins in Lipid Environments**, California Breast Cancer Research Program Symposium BB-3, San Diego, CA.

Marassi F.M., Choi J., Gong X.-M., Zhai D., and Reed J.C. (2004). **NMR structures of membrane-bound Bcl-2 family proteins**. Keystone Symposium: Apoptosis in Biochemistry and Structural Biology, Poster 223, Keystone, CO.

Funding applied for, based on work supported by this award.

R01GM65374 (Marassi) 12/01/04 - 11/30/09 $200,000 Annual Direct

National Institutes of Health / NIGMS

Structures of the Membrane-associated Bcl-2 Apoptotic Proteins.

The aims are to: (1) Characterize the topology of membrane-associated Bcl2 proteins; (2) Determine the structures of the membrane-associated Bcl2 proteins; and (3) Test the functions of wild-type and mutant Bcl2 proteins. The structures are determined using NMR on samples of Bcl2 in lipid micelles and bilayers.

R21AI063563 (Marassi) 12/01/04 - 11/30/06 Annual Direct: $137,500

National Institutes of Health / NIAID

Bim structure and apoptosis.

The aims are to: (1) Develop the expression and NMR sample preparation of pro-apoptotic Bim; (2) Perform the initial NMR experiments for the structure determination of Bim; and (3) Characterize the biological activity of Bim.

BC044465 (Marassi) 12/01/04 - 11/30/07 Annual Direct: $100,000

Department of Defense Breast Cancer Research Program

Structure and function of the cell death promoter protein Bim: role in breast cancer and apoptosis.

The aims are to: (1) Determine the structure of the soluble form of the pro-apoptotic protein Bim, and (2) characterize its biological function.

CONCLUSIONS

Our work in the past year has enabled us to obtain the first membrane-bound structural data on the Bcl-2 protein family, using solid-state NMR in lipid bilayer samples [1, 2]. The spectra provide the first structural view of Bcl-X_L and Bid in membranes, and provide insights to their function in apoptosis regulation. We are currently working on NMR data analysis for three-dimensional structure determination, and have made additional progress in developing the methodology for NMR structure determination of membrane proteins in lipid bilayers [4]. In addition, in collaboration with John Reed, also at the Burnham Institute, we are carrying out NMR experiments to map the binding site of an apoptosis regulatory peptide on pro-apoptotic Bid. The work supported by this award and described in this report, enabled us to apply for funding from the National Institutes of Health (R01GM65374; R21AI063563) and the Department of Defense (BC044465) to extend the project to include other Bcl-2 proteins.

REFERENCES

[1] Gong, X.M., Choi, J., Franzin, C.M., Zhai, D., Reed, J.C., and Marassi, F.M. (2004). **Conformation of Membrane-associated Proapoptotic tBid**. J. Biol. Chem. *279*, 28954-28960.

[2] Franzin, C.M., Choi, J., Zhai, D., Reed, J.C., and Marassi, F.M. (2004). **Structural studies of apoptosis and ion transport regulatory proteins in membranes**. Magn. Reson. Chem. *42*, 172-179.

[3] Marassi, F.M., and Crowell, K.J. (2003). **Hydration-optimized oriented phospholipid bilayer samples for solid-state NMR structural studies of membrane proteins**. J. Magn. Reson. *161*, 64-69.

[4] Marassi, F.M., and Opella, S.J. (2003). **Simultaneous assignment and structure determination of a membrane protein from NMR orientational restraints**. Protein Sci. *12*, 403-411.

[5] Mesleh, M.F., Lee, S., Veglia, G., Thiriot, D.S., Marassi, F.M., and Opella, S.J. (2003). **Dipolar waves map the structure and topology of helices in membrane proteins**. J. Am. Chem. Soc. *125*, 8928-8935.

[6] Guo, B., Zhai, D., Cabezas, E., Welsh, K., Nouraini, S., Satterthwait, A.C., and Reed, J.C. (2003). **Humanin peptide suppresses apoptosis by interfering with Bax activation**. Nature *423*, 456-461.

APPENDIX *(The appendix material was attached to the original report and is not included with this revision, except for reprint number 1, which was in press and is now published, and reprint number 3, which acknowledges the grant and was not included in the original report).*

1. Curriculum Vitae of F. M. Marassi

2. Reprints and preprints.

1 Gong, X.M., Choi, J., Franzin, C.M., Zhai, D., Reed, J.C., and Marassi, F.M. (2004). **Conformation of Membrane-associated Proapoptotic tBid**. J. Biol. Chem. *279*, 28954-28960.

2 Franzin, C.M., Choi, J., Zhai, D., Reed, J.C., and Marassi, F.M. (2004). **Structural studies of apoptosis and ion transport regulatory proteins in membranes**. Magn. Reson. Chem. *42*, 172-179.

3. Marassi, F.M., and Opella, S.J. (2003). **Simultaneous assignment and structure determination of a membrane protein from NMR orientational restraints**. *Protein Sci. 12*, 403-411.

THE JOURNAL OF BIOLOGICAL CHEMISTRY
Vol. 279, No. 28, Issue of July 9, pp. 28954–28960, 2004
Printed in U.S.A.

Conformation of Membrane-associated Proapoptotic tBid*

Received for publication, March 30, 2004, and in revised form, April 26, 2004
Published, JBC Papers in Press, April 28, 2004, DOI 10.1074/jbc.M403490200

Xiao-Min Gong, Jungyuen Choi, Carla M. Franzin, Dayong Zhai, John C. Reed, and Francesca M. Marassi‡

From The Burnham Institute, La Jolla, California 92037

The proapoptotic Bcl-2 family protein Bid is cleaved by caspase-8 to release the C-terminal fragment tBid, which translocates to the outer mitochondrial membrane and induces massive cytochrome *c* release and cell death. In this study, we have characterized the conformation of tBid in lipid membrane environments, using NMR and CD spectroscopy with lipid micelle and lipid bilayer samples. In micelles, tBid adopts a unique helical conformation, and the solution NMR $^{1}H/^{15}N$ HSQC spectra have a single well resolved resonance for each of the protein amide sites. In lipid bilayers, tBid associates with the membrane with its helices parallel to the membrane surface and without trans-membrane helix insertion, and the solid-state NMR $^{1}H/^{15}N$ polarization inversion with spin exchange at the magic angle spectrum has all of the amide resonances centered at ^{15}N chemical shift (70–90 ppm) and ^{1}H-^{15}N dipolar coupling (0–5 kHz) frequencies associated with NH bonds parallel to the bilayer surface, with no intensity at frequencies associated with NH bonds in trans-membrane helices. Thus, the cytotoxic activity of tBid at mitochondria may be similar to that observed for antibiotic polypeptides, which bind to the surface of bacterial membranes as amphipathic helices and destabilize the bilayer structure, promoting the leakage of cell contents.

Programmed cell death is initiated when death signals activate the caspases, a family of otherwise dormant cysteine proteases. External stress stimuli trigger the ligation of cell surface death receptors, thereby activating the upstream initiator caspases, which in turn process and activate the downstream cell death executioner caspases (1). In addition, caspases can be activated when stress or developmental cues within the cell induce the release of cytotoxic proteins from mitochondria. This intrinsic mitochondrial pathway for cell death is regulated by the relative ratios of the pro- and antiapoptotic members of the Bcl-2 protein family (2).

Bcl-2 family proteins exert their apoptotic activities through binding with other Bcl-2 family members or other nonhomologous proteins and through the formation of ion-conducting pores that are thought to influence cell fate by regulating mitochondrial physiology. Their functions are also regulated by subcellular location, since they cycle between soluble and membrane-bound forms. The proteins share sequence homology in four evolutionarily conserved domains (BH1–BH4), of which the BH3 domain is highly conserved and essential for both cell killing and oligomerization among Bcl-2 family members. The antiapoptotic family members have all four domains, whereas all of the proapoptotic members lack BH4, and some only have BH3. These BH3-only proteins are activated by upstream death signals, which trigger their transcriptional induction or post-translational modification, providing a key link between the extrinsic death receptor and intrinsic mitochondrial pathways to cell death (3).

One of these BH3-only Bcl-2 family members, Bid, is a 195-residue cytosolic protein that lacks the hydrophobic C-terminal domain often found in other Bcl-2 family members and connects the extrinsic and intrinsic cell death pathways (4). The major mechanism for Bid activation involves its cleavage by caspase-8, after engagement of the Fas or TNFR1 cell surface receptors (5–7). Caspase-8 cleavage of Bid releases the 15-kDa C-terminal fragment tBid, which translocates to the outer mitochondrial membrane, where it induces massive cytochrome *c* release and cell death. tBid has a 10-fold greater binding affinity for its antagonist Bcl-X_L and is 100-fold more efficient in inducing cytochrome-c release from mitochondria than its full-length precursor. Upon translocation from the cytosol to mitochondria, tBid can interact with proapoptotic Bax and Bak to promote mitochondrial apoptosis (8, 9), or it can interact with antiapoptotic Bcl-2 and Bcl-X_L and, thus, be sequestered from the cell and held in check (10). Cell-free studies have shown that Bid and Bax are sufficient to form large openings in reconstituted lipid vesicles (11). In addition, tBid can promote the alteration of membrane curvature in artificial lipid bilayers (12), and it can associate directly with mitochondria, inducing a remodeling of mitochondrial structure. tBid-induced mitochondrial remodeling is characterized by the reorganization of inner membrane cristae to form a highly interconnected common intermembrane space and is accompanied by redistribution of the cytochrome *c* stores from individual cristae to the intermembrane space (13), which may account for the rapid and complete release of mitochondrial cytochrome *c* that is observed in the presence of tBid.

The Bid BH3 domain, while essential for binding to other Bcl-2 family members, is not required for either translocation to the outer mitochondrial membrane and mitochondrial remodeling or complete cytochrome *c* release. The specific targeting of tBid to the outer mitochondrial membrane is mediated by the abundant mitochondrial lipid cardiolipin (14, 15), whose metabolism further regulates cytochrome *c* release and mitochondrion-dependent apoptosis in a Bcl-2- and caspase-independent manner (16).

* This research was supported by Department of the Army Breast Cancer Research Program Grants DAMD17-00-1-0506 and DAMD17-02-1-0313 (to F. M. M.), California Breast Cancer Research Program Grant 8WB0110 (to F. M. M.), and National Institutes of Health Grant R01GM60554 (to J. C. R.). The NMR studies utilized the Burnham Institute NMR Facility, supported by National Institutes of Health Grant P30CA30199 and the Biomedical Technology Resources for Solid-State NMR of Proteins at the University of California San Diego, supported by National Institutes of Health Grant P41EB002031. The costs of publication of this article were defrayed in part by the payment of page charges. This article must therefore be hereby marked "*advertisement*" in accordance with 18 U.S.C. Section 1734 solely to indicate this fact.

‡ To whom correspondence should be addressed: The Burnham Institute, 10901 N. Torrey Pines Rd., La Jolla, CA 92037. Tel.: 858-713-6282; Fax: 858-713-6268; E-mail: fmarassi@burnham.org.

These lines of evidence suggest that Bid induces cell death through two separate mechanisms, a BH3-dependent mechanism that involves binding to other multidomain Bcl-2 family members and a BH3-independent mechanism that involves direct association and interaction with the outer mitochondrial membrane.

The structure of full-length Bid in solution consists of eight α-helices arranged with two central somewhat more hydrophobic helices forming the core of the molecule (17, 18). The third helix, which contains the BH3 domain, is connected to the first two helices by a long flexible loop, which includes the caspase-8 cleavage site, Asp^{60} (Fig. 1). Despite the lack of sequence homology, the structure of Bid is strikingly similar to those of other anti- and proapoptotic multidomain Bcl-2 family proteins (19–22), and it is also similar to the structure of the pore-forming domains of bacterial toxins. Indeed, like the toxins and other Bcl-2 family proteins, tBid also forms ion-conducting pores in lipid bilayers (23). The structural basis for Bcl-2 pore formation is not known, since the structures that have been determined are for the soluble forms of the proteins, but by analogy to the bacterial toxins, the Bcl-2 pores are thought to form by a rearrangement of their compactly folded helices upon contact with the mitochondrial membrane. One model proposes membrane insertion of the core hydrophobic helical hairpin with the other helices folding up to rest on the membrane surface, whereas an alternative model envisions the helices rearranging to bind the membrane surface without insertion (24, 25).

In this study, we have examined the conformation and topology of tBid in lipid membrane environments, using solution NMR and CD experiments with micelle samples and solid-state NMR experiments with lipid bilayer samples. In the absence of lipids, tBid is soluble and retains a largely helical conformation, but many of the $^1H/^{15}N$ resonances are missing from the solution NMR heteronuclear single quantum coherence (HSQC)[1] spectrum, suggesting that tBid aggregates, adopts multiple conformations, or undergoes dynamic averaging on the NMR time scale. In micelles, tBid adopts a unique helical conformation, reflected in the HSQC spectrum, where each of the 130 amide sites gives rise to a single well resolved resonance. The solid-state NMR polarization inversion with spin exchange at the magic angle (PISEMA) spectrum of tBid in lipid bilayers demonstrates that it binds the membrane with its helices parallel to the membrane surface and without transmembrane helix insertion. This suggests that the BH3-independent cytotoxic activity of tBid may be similar to that observed for antibiotic polypeptides that bind to the surface of bacterial membranes as amphipathic helices and destabilize the bilayer structure, promoting the leakage of cell contents.

MATERIALS AND METHODS

Protein Expression—The gene encoding human tBid was obtained by PCR amplification of the 405-base pair segment corresponding to amino acids 60–195 of full-length human Bid (accession number P55957). The gene was cloned into the pMMHa vector, which directs the expression of proteins fused to the C terminus of the His_9-TrpΔLE polypeptide (26). The plasmid was transformed in *Escherichia coli* C41(DE3), a mutant strain that was selected for the expression of insoluble or toxic proteins (27). tBid was expressed as an insoluble protein, with the His_9-TrpΔLE polypeptide fused to its N terminus. To enable CNBr (cyanogen bromide) cleavage of tBid from the TrpΔLE fusion partner, the Met residues (Met^{97}, Met^{142}, Met^{148}, and Met^{194}) in the tBid sequence were changed to Leu. The His_9-TrpΔLE-tBid fusion protein was purified from the inclusion body fraction of the lysate by nickel affinity chromatography (His·Bind Resin (Novagen, Madison, WI) in 6 M guanidine HCl, 20 mM Tris-Cl, pH 8.0, 500 mM NaCl, 500 mM imidazole). After dialysis against water, the fusion protein was dissolved in 0.1 N HCl and then cleaved from the TrpΔLE fusion partner by reaction with a 10-fold molar excess of CNBr (28). tBid was purified by reverse-phase high pressure liquid chromatography (Delta-Pak C4 (Waters, Milford, MA) in 50% water, 50% acetonitrile, 0.1% trifluoroacetic acid). The methods for inclusion bodies isolation and fusion protein purification were as described (26, 29). Cell cultures were in M9 minimal medium as described (29). For the production of uniformly ^{15}N-labeled proteins, $(^{15}NH_4)_2SO_4$ was supplied as the sole nitrogen source. For selectively labeled protein, individual ^{15}N-labeled and nonlabeled amino acids were provided. All isotopes were from Cambridge Isotope Laboratories (Andover, MA).

Mitochondrial Release Assays—HeLa cells were harvested and then washed and suspended in HM buffer (10 mM HEPES, pH 7.4, 250 mM mannitol, 10 mM KCl, 5 mM $MgCl_2$, 1 mM EGTA, 1 mM phenylmethylsulfonyl fluoride, and complete protease inhibitor mixture (Roche Applied Science)). Cells were homogenized with 50 strokes of a Teflon homogenizer with a B-type pestle and centrifuged twice at 600 × *g* for 5 min at 4 °C. The supernatant was centrifuged at 10,000 × *g* for 10 min at 4 °C, and the resulting pellet, containing mitochondria, was washed twice in HM buffer and then suspended in HM buffer at a concentration of 1 mg/ml. Isolated HeLa mitochondria (10 μl) were incubated with HM buffer (50 μl) containing increasing amounts of tBid at 30 °C for 1 h. The samples were centrifuged at 10,000 × *g* for 10 min, and the pellet and supernatant fractions were each resolved by SDS-PAGE and analyzed by immunoblotting using cytochrome *c* and second mitochondria-derived activator of caspases (SMAC) antibodies.

Bcl-X_L Binding Assays—The expression of recombinant His-tagged Bcl-X_L(ΔC), without the C-terminal amino acids 212–233, was as described (30). For the binding assays, His_6-Bcl-X_L(ΔC) protein (15 μg) was incubated at 4 °C for 4 h with 10 μl of Ni^{2+}-NTA resin (Novagen, Madison, WI) in phosphate-buffered saline buffer (10 mM sodium phosphate, 150 mM sodium chloride, pH 7.2), and then the resin was washed three times, tBid (15 μg) was added, and the mixture was further incubated for 4 h. The resin was washed three times with phosphate-buffered saline, and then the bound proteins were eluted with 500 mM imidazole. The samples were resolved by SDS-PAGE stained with Coomassie Blue. As a control, tBid was incubated with the resin in the absence of Bcl-X_L.

CD Spectroscopy—The samples were identical to those used for solution NMR experiments but contained 40 μM tBid. The samples were transferred to a quartz cuvette (0.1-mm path length), and far-UV CD spectra were recorded at 25 °C on a model 62A-DS CD spectrometer (Aviv, Lakewood, NJ) equipped with a temperature controller. A 5-s time constant and a 1-nm bandwidth were used during data acquisition over a wavelength range of 180–260 nm. For each sample, three spectra were recorded, averaged, and referenced by subtracting the average of three spectra obtained using the buffer alone. The spectra were analyzed for protein secondary structure with the k2d program (available on the World Wide Web at www.embl-heidelberg.de/~andrade/k2d/) (31).

Solution NMR—The sample of tBid without lipids contained 0.7–1 mM ^{15}N-labeled tBid, in 50 mM sodium phosphate, pH 5. In the absence of lipids, tBid is not soluble in the millimolar concentrations required for NMR at pH values greater than 5. The samples of tBid in micelles contained 1 mM ^{15}N-labeled tBid in 20 mM sodium phosphate, pH 7, with 500 mM SDS (Cambridge, Andover, MA) or 100 mM 1-palmitoyl-2-hydroxy-*sn*-glycero-3-[phospho-*rac*-(1-glycerol)] (LPPG); Avanti, Alabaster, AL).

Solution NMR experiments were performed on a Bruker AVANCE 600 spectrometer (Billerica, MA) with a 600/54 Magnex magnet (Yarnton, UK), equipped with a triple-resonance 5-mm probe with three-axis field gradients. The two-dimensional $^1H/^{15}N$ HSQC (32) spectra were obtained at 40 °C. The ^{15}N and ^1H chemical shifts were referenced to 0 ppm for liquid ammonia and tetramethylsilane, respectively. The NMR data were processed using NMR Pipe and rendered in NMR Draw (33) on a Dell Precision 330 MT Linux work station (Round Rock, TX).

Solid-state NMR—The lipids, 1,2-dioleoyl-*sn*-glycero-3-phosphocholine (DOPC) and 1,2-dioleoyl-*sn*-glycero-3-[phospho-*rac*-(1-glycerol)] (DOPG) were from Avanti (Alabaster, AL). Samples of tBid in lipid bilayers were prepared by mixing 5 mg of ^{15}N-labeled tBid in water with 100 mg of lipids (DOPC/DOPG, 6:4 molar ratio) that had been sonicated in water to form unilamellar vesicles. The protein and lipid vesicle mixture was incubated on ice for 30 min and then distributed onto the

[1] The abbreviations used are: HSQC, heteronuclear single quantum coherence; PISEMA, polarization inversion with spin exchange at the magic angle; SMAC, second mitochondria-derived activator of caspases; NTA, nitrilotriacetic acid; DOPC, 1,2-dioleoyl-*sn*-glycero-3-phosphocholine; DOPG, 1,2-dioleoyl-*sn*-glycero-3-[phospho-*rac*-(1-glycerol)]; LPPG, 1-palmitoyl-2-hydroxy-*sn*-glycero-3-[phospho-*rac*-(1-glycerol)].

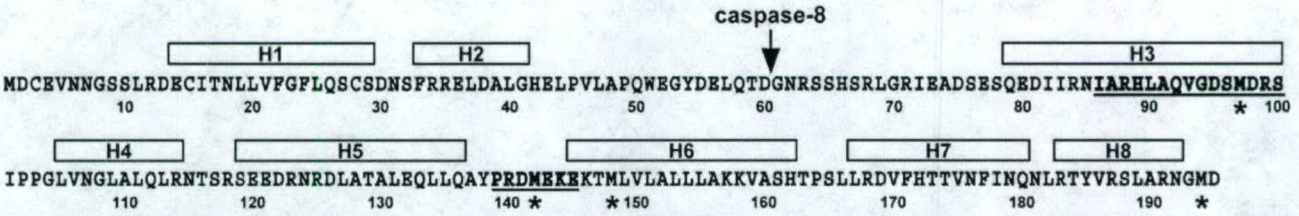

FIG. 1. **Amino acid sequence of human Bid (accession number P55957).** The eight helices (H1–H8) are those determined in the solution NMR structure of full-length human Bid (Protein Data Bank number 2BID) (17). The central core helices are H6 and H7. The BH3 domain in H3 and the putative lipid binding motif before H6 are in *boldface type* and *underlined*. The *arrow* marks the caspase-8 cleavage site at Asp^{60}, and the sequences of both wild-type and recombinant tBid start at Gly^{61}. The *asterisks* mark the four Met residues that were mutated to Leu in recombinant tBid.

surface of 15 glass slides (11 × 11 × 0.06 mm; Marienfeld, Germany). After allowing excess water to evaporate at 40 °C, the slides were stacked and equilibrated for 12 h at 40 °C and 93% relative humidity, in order to form oriented lipid bilayers. The samples were wrapped in parafilm and then sealed in thin polyethylene film prior to insertion in the NMR probe. Hydrogen-exchanged samples were prepared by exposing the stacked oriented bilayer samples to an atmosphere saturated with D_2O.

Solid-state NMR experiments were performed on a Bruker AVANCE 500 spectrometer (Billerica, MA) with a 500/89 AS Magnex magnet (Yarnton, UK). The home-built $^1H/^{15}N$ double resonance probe had a square radiofrequency coil (11 × 11 × 3 mm) wrapped directly around the samples. The one-dimensional ^{15}N chemical shift spectra were obtained with single contact cross-polarization with mismatch-optimized IS polarization transfer (34, 35). The two-dimensional spectra that correlate ^{15}N chemical shift with ^1H-^{15}N dipolar coupling were obtained with PISEMA (36). The spectra were obtained with a cross-polarization contact time of 1 ms, a ^1H 90° pulse width of 5 μs, and continuous ^1H decoupling of 63-kHz radio frequency field strength. The two-dimensional data were acquired with 512 accumulated transients and 256 complex data points, for each of 64 real t1 values incremented by 32.7 μs. The recycle delay was 6 s. The ^{15}N chemical shifts were referenced to 0 ppm for liquid ammonia. The data were processed using NMR Pipe and rendered in NMR Draw (33) on a Dell Precision 330 MT Linux work station (Round Rock, TX).

Calculation of Solid-state NMR Spectra—Two-dimensional $^1H/^{15}N$ PISEMA spectra were calculated on a Linux Dell computer as described previously (37). The ^{15}N chemical shift and ^1H-^{15}N dipolar coupling frequencies were calculated for various orientations of an 18-residue α-helix, with 3.6 residues per turn and uniform backbone dihedral angles for all residues ($\phi = -57°$; $\psi = -47°$). The principal values and molecular orientation of the ^{15}N chemical shift tensor (σ_{11} = 64 ppm; σ_{22} = 77 ppm; σ_{33} = 217 ppm; angle (σ_{11}NH) = 17°) and the NH bond distance (1.07 Å) provided the input for the spectrum calculation at each helix orientation.

RESULTS

Protein Expression and Biological Activity—Full-length Bid can be expressed at high levels, in *E. coli*, as a soluble protein, but tBid overexpression is toxic for bacterial cells. To produce milligram quantities of ^{15}N-labeled tBid for NMR studies, we used the pMMHa fusion protein vector that directs high level protein expression as inclusion bodies, and we transformed the plasmid in *E. coli* C41(DE3) cells, selected for the expression of insoluble and toxic proteins (27). tBid was separated from the fusion partner by means of CNBr cleavage at the engineered N-terminal Met residue (26). This method yields ~10 mg of purified ^{15}N-labeled tBid from 1 liter of culture. To avoid cleavage within the tBid segment, the four Met residues in the tBid amino acid sequence were mutated to Leu (Fig. 1, *asterisks*), and therefore, it was important to demonstrate that the recombinant protein retained its biological activity.

We tested the ability of recombinant tBid to induce the release of mitochondrial proteins by incubating it with mitochondria isolated from HeLa cells, assaying the supernatant and pelleted fractions with antibodies to cytochrome *c* and SMAC. Fig. 2*A* demonstrates that, in both cases, tBid is fully active, in a dose-dependent manner and at levels similar to wild-type tBid obtained by caspase-8 cleavage (38). Next we

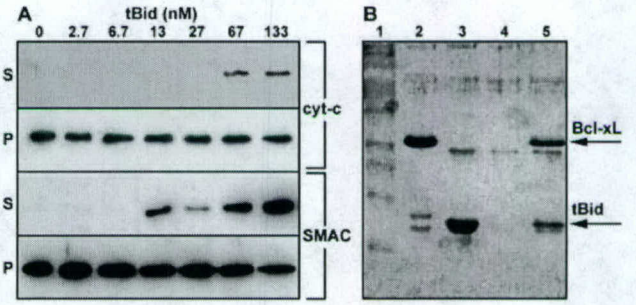

FIG. 2. **Recombinant tBid induces the release of cytochrome-c and SMAC from isolated mitochondria and binds to Bcl-X_L *in vitro*.** *A*, isolated HeLa mitochondria (10 μl, 1 mg/ml) were incubated with increasing amounts (0–133 nM in 50 μl) of tBid. The supernatant (*S*) and pellet (*P*) fractions were separated by centrifugation, resolved on SDS-PAGE, and analyzed by Western blotting with either cytochrome *c* (*top*) or SMAC (*bottom*) antibody. In *B*, Ni^{2+}-NTA resin (10 μl) was incubated first with His-Bcl-X_L(ΔC) (15 μg) and then with tBid (15 μg). The Ni^{2+}-NTA-bound protein was eluted with 500 mM imidazole, and the samples were resolved by SDS-PAGE and stained with Coomassie Blue (*lane 5*). In the control experiment, tBid was directly incubated with the resin without preincubation with Bcl-X_L(ΔC) (*lane 4*). Individual Bcl-X_L(ΔC) monomers (24 kDa) are resolved in *lane 2*, and individual tBid monomers (15 kDa) are resolved in *lane 3*. Molecular weight markers are shown in *lane 1*.

tested the ability of recombinant tBid to bind Bcl-X_L, since this interaction requires the BH3 domain, and recombinant tBid contains the mutation M97L in this segment. When recombinant tBid, which does not have a His tag, was incubated with Ni^{2+}-NTA without Bcl-X_L, it did not bind the resin, as evidenced by the absence of tBid in the imidazole elution (Fig. 2*B*, *lane 4*). However, when tBid was incubated with Ni^{2+}-NTA that had been previously incubated with His-tagged Bcl-X_L, it also bound to the resin and eluted with Bcl-X_L in imidazole (Fig. 2*B*, *lane 5*).

Thus, we conclude that recombinant tBid, isolated from inclusion bodies, is fully active in its ability to induce cytochrome *c* and SMAC release from isolated mitochondria and that its capacity to bind antiapoptotic Bcl-X_L through its BH3 domain is not disrupted by the M97L mutation. The pMMHa vector may be generally useful for the high level expression of other proapoptotic proteins that are difficult to express because of their cytotoxic properties. The use of chemical cleavage eliminates the difficulties, poor specificity, and enzyme inactivation, often encountered with protease treatment of insoluble proteins, and in cases where Met mutation is not feasible, protein cleavage from the fusion partner can be obtained enzymatically by engineering specific protease cleavage sites for the commonly used enzymes thrombin, Fxa, enterokinase, and tobacco etch virus protease. Thrombin and tobacco etch virus retain activity in the presence of detergents, including low millimolar concentrations of SDS.

tBid in Lipid Micelles—The cleavage of Bid by caspase-8

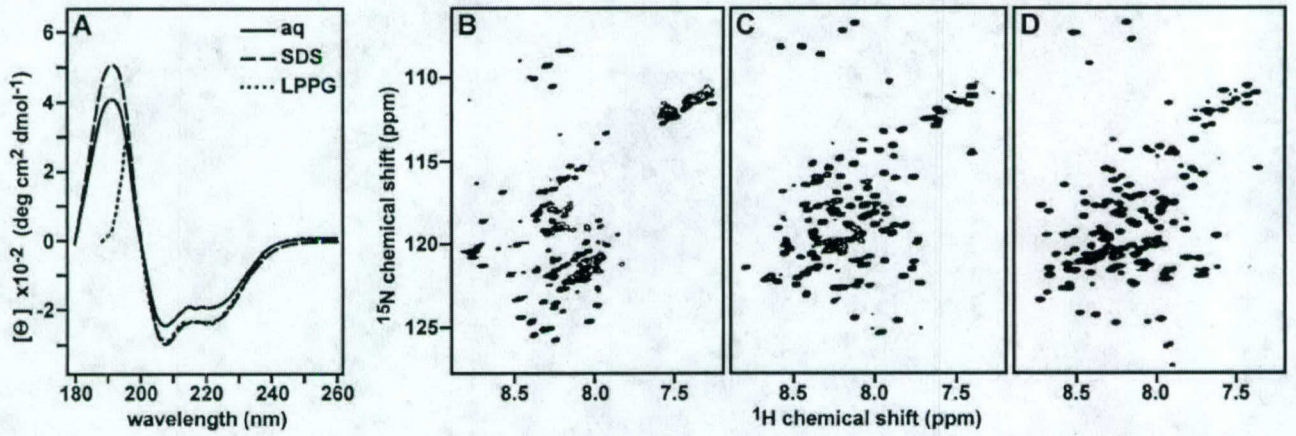

FIG. 3. **tBid adopts a helical fold in lipid micelles.** The CD spectra in *A* were obtained at 25 °C for tBid in aqueous solution (*solid line*), SDS micelles (*broken line*), or LPPG micelles (*dotted line*). The $^{1}H/^{15}N$ HSQC NMR spectra in *B–D* were obtained at 40 °C for uniformly ^{15}N-labeled tBid, in aqueous solution (*B*), SDS micelles (*C*), or LPPG micelles (*D*). Aqueous samples were in 20 mM sodium phosphate, pH 5; SDS micelle samples were in 20 mM sodium phosphate, pH 7, 500 mM SDS; and LPPG micelle samples were in 20 mM sodium phosphate, pH 7, 100 mM LPPG.

results in a C-terminal product, tBid, which targets mitochondria and induces apoptosis with strikingly enhanced activity (5–7). To characterize the conformation of tBid in lipid environments, we obtained its CD and solution NMR $^{1}H/^{15}N$ HSQC spectra in the absence or in the presence of lipid micelles (Fig. 3). The HSQC spectra of proteins are the starting point for additional multidimensional NMR experiments that lead to structure determination. In these spectra, each ^{15}N-labeled protein site gives rise to a single peak, characterized by ^{1}H and ^{15}N chemical shift frequencies that reflect the local environment. In addition, the peak line widths and line shapes and their dispersion in the ^{1}H and ^{15}N frequency dimensions reflect protein conformation and aggregation state.

In the absence of lipids, the CD spectrum of tBid displays minima at 202 and 222 nm, characteristic of predominantly helical proteins (Fig. 3*A*, *solid line*). The helical content estimated from the CD spectrum is ~65%, which is similar to the 67% helical content determined from the three-dimensional structure of Bid (17) for the 135 C-terminal amino acids that correspond to tBid. However, whereas tBid retains its helical conformation even when it is separated from the 60-residue N-terminal fragment, many of the resonances in its $^{1}H/^{15}N$ HSQC spectrum cannot be detected (Fig. 3*B*), suggesting that the protein aggregates in solution, adopts multiple conformations, or undergoes dynamic conformational exchange on the NMR time scale. tBid has very limited solubility at pH values greater than 5, and the addition of KCl up to 200 mM did not improve the appearance of the HSQC spectrum, whereas KCl concentrations above 200 mM yielded a gel. This behavior is consistent with the dramatic changes in the physical properties of the protein that accompany caspase-8 cleavage. Bid has a theoretical pI of 5.3 and a net charge of −7, but caspase-8 cleavage and removal of the 60 N-terminal amino acids shift these parameters to the opposite end of their spectrum, and tBid has a pI of 9.3 and a net charge of +2. In addition, the removal of helix-1 and helix-2 following caspase-8 cleavage exposes hydrophobic residues in the BH3 domain in helix-3 and in the central core helices, helix-6 and helix-7 (17, 18, 23).

When tBid associates with lipid micelles, its HSQC spectrum changes dramatically, and single, well defined $^{1}H/^{15}N$ resonances are observed for each ^{15}N-labeled NH site in the protein, indicating that tBid adopts a unique conformation in this environment (Fig. 3, *C* and *D*). Micelles provide suitable membrane mimetic samples for solution NMR studies of membrane proteins and a realistic alternative to organic solvents, because their small size affords rapid and effectively isotropic reorientation of the protein and because their amphipathic nature simulates that of membranes. The principle goal of micelle sample preparation is to reduce the effective rotational correlation time of the protein so that resonances will have the narrowest achievable line widths while providing an environment that maintains the protein fold.

Several lipids are available for protein solubilization, and we tested both SDS (Fig. 3*C*) and LPPG (Fig. 3*D*) for their ability to yield high quality HSQC spectra of tBid for structure determination. Both gave excellent spectra where most of the 130 tBid amide resonances could be resolved. Both SDS and LPPG are negatively charged, but they differ substantially in the lengths of their hydrocarbon chains (C12 for SDS; C16 for LPPG) and their polar headgroups (sulfate for SDS; phosphatidylglycerol for LPPG); thus, the differences in ^{1}H and ^{15}N chemical shifts between the two HSQC spectra most likely reflect the different lipid environments. The spectrum in LPPG has exceptionally well dispersed resonances with homogeneous intensities and line widths. LPPG was recently identified as a superior lipid for NMR studies of several membrane proteins (39) and is particularly interesting for this study because it is a close analog of cardiolipin and monolysocardiolipin, the major components of mitochondrial membranes that bind tBid (14).

In both the SDS and LPPG spectra, the limited chemical shift dispersion is typical of helical proteins in micelles, and this is confirmed by the corresponding CD spectra, which are dominated by minima at 202 and 222 nm, and thus show that tBid retains a predominantly helical fold in both types of micelles (Fig. 3*A*, *broken* and *dotted lines*). We estimated the helical content of tBid in lipid micelles to be ~65%, similar to that of tBid in the absence of lipids and to the value determined for the 135-residue C-terminal segment in the three-dimensional solution structure of Bid (17).

tBid in Lipid Bilayers—By analogy to the structurally homologous colicin and diphtheria bacterial toxins, the mechanism of pore formation by tBid has been thought to involve insertion through the membrane of the two central core helices, helix-6 and helix-7 (23, 25). To examine the conformation of tBid associated with membranes, we obtained one-dimensional ^{15}N chemical shift and two-dimensional $^{1}H/^{15}N$ PISEMA solid-state NMR spectra of ^{15}N-labeled tBid reconstituted in lipid bilayers (Fig. 4). In these samples, the lipid composition of 60% DOPC and 40% DOPG was chosen to mimic the highly negative charge of mitochondrial membranes. This lipid composition is

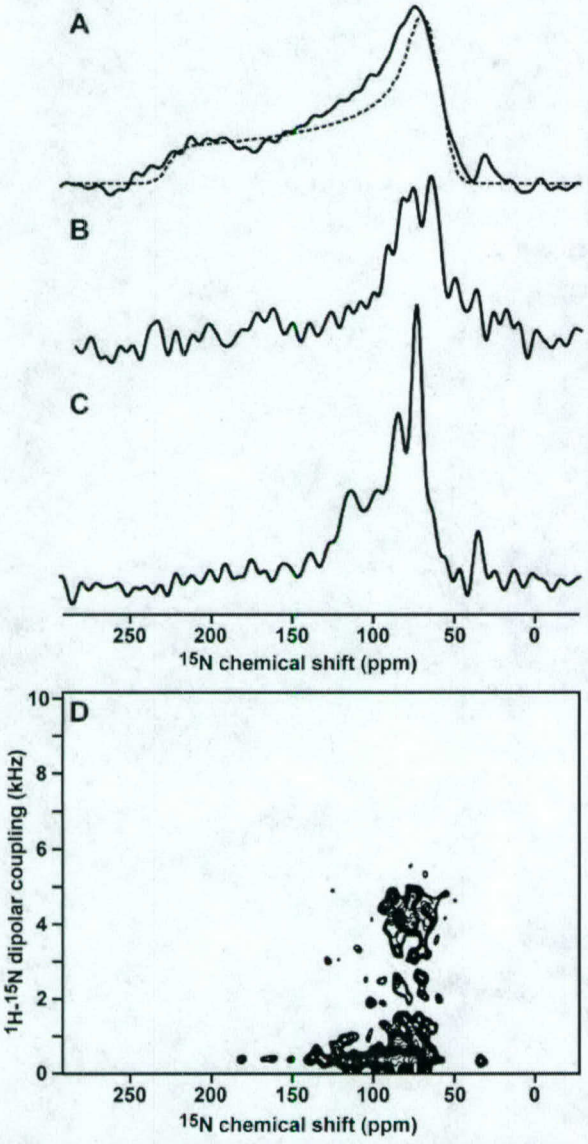

FIG. 4. **Solid-state NMR spectra of tBid in lipid bilayers show that tBid binds membranes with a unique fold and parallel orientation.** *A*, one-dimensional ^{15}N chemical shift spectrum of uniformly ^{15}N-labeled tBid in unoriented lipid bilayer vesicles (*solid line*) and powder pattern calculated for a rigid ^{15}N amide site (*dotted line*). *B*, one-dimensional ^{15}N spectrum of selectively ^{15}N-Lys-labeled tBid in oriented lipid bilayers. *C*, one-dimensional ^{15}N spectrum of uniformly ^{15}N-labeled tBid in oriented lipid bilayers. *D*, two-dimensional ^{1}H/^{15}N PISEMA spectrum of tBid in oriented lipid bilayers.

identical to that of the liposomes used for the measurement of the ion channel activities of Bid and tBid (23), and since the oriented lipid bilayers used in this study were obtained from liposomes prepared in the same way as for the channel studies, the NMR spectra obtained in this work represent the channel-active conformation of tBid.

When the lipid bilayers are oriented with their surface perpendicular to the magnetic field, the solid-state NMR spectra of the membrane-associated proteins trace out maps of their structure and orientation within the membrane and thus provide very useful structural information prior to complete structure determination. For example, helices give characteristic solid-state NMR spectra where the resonances from amide sites in the protein trace-out helical wheels that contain information about helix tilt and rotation within the membrane (37, 40, 41). Typically, trans-membrane helices have PISEMA spectra with ^{15}N chemical shifts between 150 and 200 ppm, and ^{1}H-^{15}N dipolar couplings between 2 and 10 kHz, whereas helices that bind parallel to the membrane surface have spectra with shifts between 70 and 100 ppm and couplings between 0 and 5 kHz. We refer to these as the trans-membrane and in-plane regions of the PISEMA spectrum, respectively.

The ^{15}N chemical shift spectrum of tBid in unoriented lipid bilayer vesicles is a powder pattern (Fig. 4*A*, *solid line*) that spans the full range (60–220 ppm) of the amide ^{15}N chemical shift interaction (Fig. 4*A*, *dotted line*). The absence of additional intensity at the isotropic resonance frequencies (100–130 ppm) demonstrates that the majority of amino acid sites are immobile on the time scale of the ^{15}N chemical shift interaction, although it is possible that some mobile unstructured residues cannot be observed by cross-polarization. The peak at 35 ppm is from the amino groups at the N terminus and side chains of the protein.

The spectrum of tBid in planar oriented lipid bilayers is very different (Fig. 4*C*). The amide resonances are centered at a frequency associated with NH bonds in helices parallel to the membrane surface (80 ppm), whereas no intensity is observed at frequencies associated with NH bonds in trans-membrane helices (200 ppm). The resonances near 120 ppm are unlikely to result from mobile sites, since little or no isotropic intensity is observed in the spectrum from unoriented bilayers; instead, they probably reflect specific orientations of their corresponding sites near the magic angle, which corresponds to 35.3° from the membrane surface. The NMR data show no evidence of conformational exchange on the millisecond to second time scale of the channel opening and closing events, excluding the possibility of transient insertion of tBid in the membrane. Therefore, we conclude that tBid binds strongly to the membrane surface, adopting a unique conformation and orientation in the presence of phospholipids.

Amide hydrogen exchange rates are useful for identifying residues that are involved in hydrogen bonding and that are exposed to water. The amide hydrogens in trans-membrane helices can have very slow exchange rates due to their strong hydrogen bonds in the low dielectric of the lipid bilayer environment, and their ^{15}N chemical shift NMR signals persist for days after exposure to D_2O (42). On the other hand, trans-membrane helices that are in contact with water because they participate in channel pore formation and other water-exposed helical regions of proteins have faster exchange rates, and their NMR signals disappear on the order of hours (43). To examine the amide hydrogen exchange rates for membrane-bound tBid, we obtained solid-state NMR spectra after exposing the oriented lipid bilayer sample to D_2O for 2, 5, and 7 h. The majority of resonances in the ^{15}N chemical shift spectrum of tBid disappeared within 7 h, indicating that the amide hydrogens exchange and, hence, are in contact with the lipid bilayer interstitial water.

The tBid amino acid sequence has four Lys residues (Lys^{144}, Lys^{146}, Lys^{157}, and Lys^{158}), all located in or near helix-6, one of the two helices thought to insert in the membrane and form the tBid ion-conducting pore. The spectrum of ^{15}N-Lys-labeled tBid in bilayers is notable because its amide resonances all have chemical shifts near 80 ppm, in the in-plane region of the spectrum, and this cannot be reconciled with membrane insertion (Fig. 4*B*). Since tBid maintains a helical fold in lipid micelles and it is reasonable to assume that the helix boundaries are not appreciably changed from those of full-length Bid, the solid-state NMR data demonstrate that helix-6 does not insert through the membrane but associates parallel to its surface. This is also supported by recent EPR data (44).

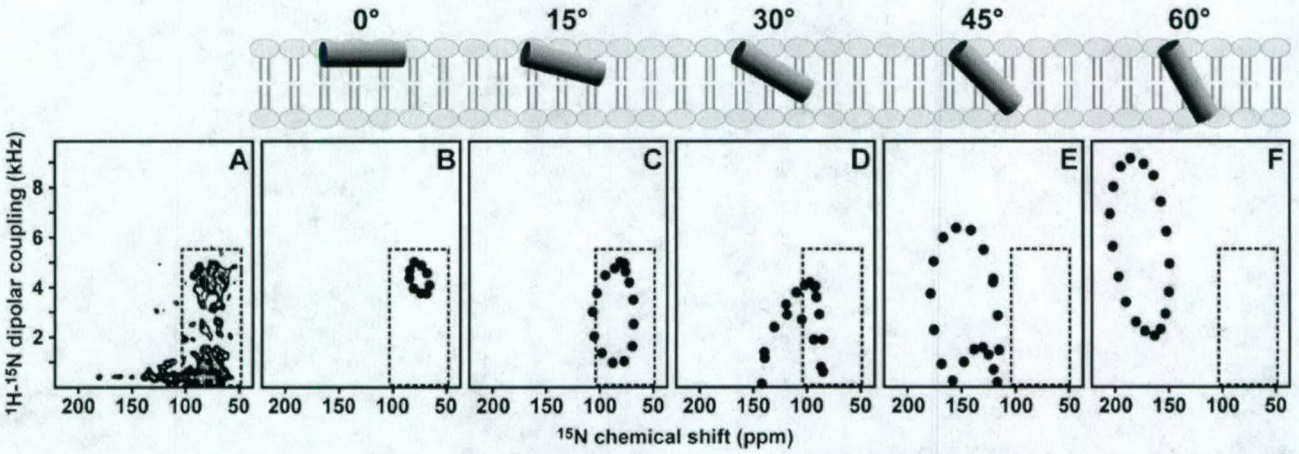

FIG. 5. **Two-dimensional solid-state NMR ^{1}H/^{15}N PISEMA spectrum of uniformly ^{15}N-labeleld tBid in oriented lipid bilayers.** The experimental spectrum (*A*) is compared with the theoretical spectra (*B–F*) calculated for an 18-residue α-helix, with uniform backbone dihedral angles ($\phi = -57°$; $\psi = -47°$) and different helix tilts (0–60°) relative to the membrane surface, as depicted in the *schematic diagrams above* the *spectra*. The 0° orientation is for a helix parallel to the membrane surface.

These findings are confirmed and refined with the two-dimensional ^{1}H/^{15}N PISEMA spectrum of tBid in bilayers (Fig. 4*D*). Each amide site in the protein contributes one correlation peak, characterized by ^{1}H-^{15}N dipolar coupling and ^{15}N chemical shift frequencies that reflect NH bond orientation relative to the membrane. For tBid, the circular wheel-like pattern of resonances in the spectral region bounded by 0–5 kHz and 70–90 ppm provides definitive evidence that tBid associates with the membrane as surface-bound helices without transmembrane insertion. The substantial peak overlap reflects a similar orientation of the tBid helices parallel to the membrane, and spectral resolution in this region requires three-dimensional correlation spectroscopy and selective isotopic labeling (45).

Since the NMR frequencies directly reflect the angles between individual bonds and the direction of the applied magnetic field, it is possible to calculate solid-state NMR spectra for specific models of proteins in oriented samples. For example, the spectra of helices have wheel-like patterns of resonances, called *Pisa Wheels*, that mirror helix tilt and rotation in the membrane (37, 40, 41), and a comparison of calculated and experimental spectra provides very useful structural information prior to complete structure determination. The spectra calculated for several orientations of an ideal 18-residue helix, with 3.6 residues per turn and identical backbone dihedral angles for all residues (ϕ, $\psi = -57°$, $-47°$), are shown in Fig. 5 (*B–F*) and are compared with the experimental PISEMA spectrum obtained for tBid in oriented bilayers, in Fig. 5*A*. In each spectrum, the characteristic *Pisa Wheel* pattern reflects helix tilt, but only the spectra calculated for membrane surface helices, with tilts from 0 to 15°, have intensity in the region of the experimental spectrum of tBid (*inset box*), whereas trans-membrane helices with tilts ranging from 45 to 90° from the membrane surface, have *Pisa Wheels* in a completely unpopulated region of the experimental spectrum. Based on this comparative analysis, we estimate that the helices of tBid are nearly parallel to the lipid bilayer plane (0° orientation), with tilts of no more than 20° from the membrane surface.

DISCUSSION

The results of this study demonstrate that tBid adopts a unique helical fold in lipid environments and that it binds the membrane without insertion of its helices. Solid-state NMR studies of the antiapoptotic Bcl-2 family member, Bcl-X_L, also indicate that membrane insertion of the Bcl-X_L helices is limited (42), and solution NMR studies show that Bcl-X_L adopts an extended helical conformation in lipid micelles (46). Both tBid and Bcl-X_L form ion-conductive pores that are thought to play a role in apoptosis through their regulation of mitochondrial physiology (23, 25), and since the samples in both the solid-state NMR and ion channel activity studies of tBid were identical in their lipid composition and the manner of sample preparation (23), the membrane surface association of tBid, observed by solid-state NMR in this study, is very likely to represent the channel-active conformation of the protein.

Pore formation by the Bcl-2 family proteins has been thought to involve translocation of the central core helices through the membrane, and the helices of both Bid and Bcl-X_L are sufficiently long to span the lipid bilayer. However, their amphipathic character is also compatible with membrane surface association, in a manner that is reminiscent of the antimicrobial polypeptides, where binding of the polypeptide helices to the bacterial membrane surface is thought to transiently destabilize the membrane and change its morphology, inducing leakage of the cell contents, disruption of the electrical potential, and ultimately cell death (45, 47). It is notable that bacterial and mitochondrial membranes have very similar structures and surface charge and that tBid is both capable of altering bilayer curvature (12) and of remodeling the mitochondrial membrane (13), which would be sufficient to cause the release of mitochondrial cytotoxic molecules. The membrane surface association of tBid may also serve to display the BH3 domain on the mitochondrial membrane surface, making it accessible for binding by other Bcl-2 family members.

Although tBid does not insert in DOPC/DOPG lipid bilayers, we cannot exclude the possibility that trans-membrane insertion may be driven by the presence of natural mitochondrial lipids, such as cardiolipin and monolysocardiolipin. These lipids both bind tBid (14) and are concentrated at mitochondrial outer-inner membrane contact sites where tBid localizes; however, a recent EPR study using these lipids also found no evidence of tBid helix insertion through the membrane (44). It is also possible that trans-membrane insertion of tBid requires post-translational N-terminal myristoylation, since this has been shown to enhance Bid-induced cytochrome *c* release and apoptosis (48), and that the interactions with other Bcl-2 family proteins such as Bak and Bax or with other nonhomologous proteins such as the mitochondrial voltage dependent anion channel may promote insertion of the tBid helices through the mitochondrial membrane.

Wagner and co-workers (17) monitored the solution NMR

$^{1}H/^{15}N$ HSQC spectrum of Bid after the addition of caspase-8, testing the hypothesis that Bid activation is accompanied by a conformational change. They found that the structure of Bid is not changed by caspase-8 cleavage, since tBid remains associated with the N-terminal fragment, but proposed that dissociation occurs at lower physiological concentrations, through a conformational on-off equilibrium. In light of the lipid affinity of Bid and the data in Fig. 3 demonstrating that tBid is well-folded in lipid micelles independently of the N terminus, it is possible that lipids act as a third partner during caspase-8 cleavage of Bid. Thus, whereas in the absence of lipids the two cleavage fragments remain associated, the presence of lipids may enable dissociation by providing an environment where tBid can fold independently.

In this regard, it is interesting to note that the Bid amino acid sequence (^{141}PRDMEKE^{147}) at the beginning of helix-6 is similar to the conserved sequence (^{95}PDVEKE^{100}) that forms a short lipid recognition helix in the lipoprotein apolipophorin-III. In Bid, this sequence forms a short loop that is solvent-exposed and perpendicular to the axis of helix-6, whereas in apolipophorin-III it forms a short helix at one solvent-exposed end of the molecule that is perpendicular to the helix bundle (49). This short motif is conserved in the Bid sequences from various species, suggesting that it plays a role in the protein biological function, and given the documented lipid-binding activity of Bid (14), it may constitute a lipid recognition domain for Bid similar to that of apolipophorin-III. Thus, it is possible that the structure of tBid, destabilized by dissociation from the N-terminal fragment after caspase-8 cleavage, undergoes a conformational change whereby it opens about the flexible loops that connect its helical segments to an extended helical conformation, which binds to the membrane surface. This would be similar to the mechanism proposed for apolipophorin-III, which adopts a marginally stable helix bundle topology that allows for concerted opening of the bundle about hinged loops (49).

Acknowledgment—We thank Jinghua Yu for assistance with the NMR experiments.

REFERENCES

1. Denault, J. B., and Salvesen, G. S. (2002) *Chem. Rev.* **102,** 4489–4500
2. Green, D. R., and Reed, J. C. (1998) *Science* **281,** 1309–1312
3. Cory, S., and Adams, J. M. (2002) *Natl. Rev. Cancer* **2,** 647–656
4. Wang, K., Yin, X. M., Chao, D. T., Milliman, C. L., and Korsmeyer, S. J. (1996) *Genes Dev.* **10,** 2859–2869
5. Li, H., Zhu, H., Xu, C. J., and Yuan, J. (1998) *Cell* **94,** 491–501
6. Luo, X., Budihardjo, I., Zou, H., Slaughter, C., and Wang, X. (1998) *Cell* **94,** 481–490
7. Gross, A., Yin, X. M., Wang, K., Wei, M. C., Jockel, J., Milliman, C., Erdjument-Bromage, H., Tempst, P., and Korsmeyer, S. J. (1999) *J. Biol. Chem.* **274,** 1156–1163
8. Eskes, R., Desagher, S., Antonsson, B., and Martinou, J. C. (2000) *Mol. Cell. Biol.* **20,** 929–935
9. Korsmeyer, S. J., Wei, M. C., Saito, M., Weiler, S., Oh, K. J., and Schlesinger, P. H. (2000) *Cell Death Differ.* **7,** 1166–1173
10. Cheng, E. H., Wei, M. C., Weiler, S., Flavell, R. A., Mak, T. W., Lindsten, T., and Korsmeyer, S. J. (2001) *Mol. Cell* **8,** 705–711
11. Kuwana, T., Mackey, M. R., Perkins, G., Ellisman, M. H., Latterich, M., Schneiter, R., Green, D. R., and Newmeyer, D. D. (2002) *Cell* **111,** 331–342
12. Epand, R. F., Martinou, J. C., Fornallaz-Mulhauser, M., Hughes, D. W., and Epand, R. M. (2002) *J. Biol. Chem.* **277,** 32632–32639
13. Scorrano, L., Ashiya, M., Buttle, K., Weiler, S., Oakes, S. A., Mannella, C. A., and Korsmeyer, S. J. (2002) *Dev. Cell* **2,** 55–67
14. Degli Esposti, M., Cristea, I. M., Gaskell, S. J., Nakao, Y., and Dive, C. (2003) *Cell Death Differ.* **10,** 1300–1309
15. Lutter, M., Fang, M., Luo, X., Nishijima, M., Xie, X., and Wang, X. (2000) *Nat. Cell Biol.* **2,** 754–761
16. Ostrander, D. B., Sparagna, G. C., Amoscato, A. A., McMillin, J. B., and Dowhan, W. (2001) *J. Biol. Chem.* **276,** 38061–38067
17. Chou, J. J., Li, H., Salvesen, G. S., Yuan, J., and Wagner, G. (1999) *Cell* **96,** 615–624
18. McDonnell, J. M., Fushman, D., Milliman, C. L., Korsmeyer, S. J., and Cowburn, D. (1999) *Cell* **96,** 625–634
19. Fesik, S. W. (2000) *Cell* **103,** 273–282
20. Suzuki, M., Youle, R. J., and Tjandra, N. (2000) *Cell* **103,** 645–654
21. Denisov, A. Y., Madiraju, M. S., Chen, G., Khadir, A., Beauparlant, P., Attardo, G., Shore, G. C., and Gehring, K. (2003) *J. Biol. Chem.* **278,** 21124–21128
22. Hinds, M. G., Lackmann, M., Skea, G. L., Harrison, P. J., Huang, D. C., and Day, C. L. (2003) *EMBO J.* **22,** 1497–1507
23. Schendel, S. L., Azimov, R., Pawlowski, K., Godzik, A., Kagan, B. L., and Reed, J. C. (1999) *J. Biol. Chem.* **274,** 21932–21936
24. Cramer, W. A., Heymann, J. B., Schendel, S. L., Deriy, B. N., Cohen, F. S., Elkins, P. A., and Stauffacher, C. V. (1995) *Annu. Rev. Biophys. Biomol. Struct.* **24,** 611–641
25. Schendel, S. L., Montal, M., and Reed, J. C. (1998) *Cell Death Differ.* **5,** 372–380
26. Staley, J. P., and Kim, P. S. (1994) *Protein Sci.* **3,** 1822–1832
27. Miroux, B., and Walker, J. E. (1996) *J. Mol. Biol.* **260,** 289–298
28. Gross, E., and Witkop, B. (1961) *J. Am. Chem. Soc.* **83,** 1510–1511
29. Opella, S. J., Ma, C., and Marassi, F. M. (2001) *Methods Enzymol.* **339,** 285–313
30. Xie, Z., Schendel, S., Matsuyama, S., and Reed, J. C. (1998) *Biochemistry* **37,** 6410–6418
31. Andrade, M. A., Chacon, P., Merelo, J. J., and Moran, F. (1993) *Protein Eng.* **6,** 383–390
32. Mori, S., Abeygunawardana, C., Johnson, M. O., and Vanzijl, P. C. M. (1995) *J. Magn. Reson. B* **108,** 94–98
33. Delaglio, F., Grzesiek, S., Vuister, G. W., Zhu, G., Pfeifer, J., and Bax, A. (1995) *J. Biomol. NMR* **6,** 277–293
34. Pines, A., Gibby, M. G., and Waugh, J. S. (1973) *J. Chem. Phys.* **59,** 569–590
35. Levitt, M. H., Suter, D., and Ernst, R. R. (1986) *J. Chem. Phys.* **84,** 4243–4255
36. Wu, C. H., Ramamoorthy, A., and Opella, S. J. (1994) *J. Magn. Reson. A* **109,** 270–272
37. Marassi, F. M. (2001) *Biophys. J.* **80,** 994–1003
38. Guo, B., Zhai, D., Cabezas, E., Welsh, K., Nouraini, S., Satterthwait, A. C., and Reed, J. C. (2003) *Nature* **423,** 456–461
39. Krueger-Koplin, R. D., Sorgen, P. L., Krueger-Koplin, S. T., Rivera-Torres, I. O., Cahill, S. M., Hicks, D. B., Grinius, L., Krulwich, T. A., and Girvin, M. E. (2004) *J. Biomol. NMR* **28,** 43–57
40. Marassi, F. M., and Opella, S. J. (2000) *J. Magn. Reson.* **144,** 150–155
41. Wang, J., Denny, J., Tian, C., Kim, S., Mo, Y., Kovacs, F., Song, Z., Nishimura, K., Gan, Z., Fu, R., Quine, J. R., and Cross, T. A. (2000) *J. Magn. Reson.* **144,** 162–167
42. Franzin, C. M., Choi, J., Zhai, D., Reed, J. C., and Marassi, F. M. (2004) *Magn. Reson. Chem.* **42,** 172–179
43. Tian, C., Gao, P. F., Pinto, L. H., Lamb, R. A., and Cross, T. A. (2003) *Protein Sci.* **12,** 2597–2605
44. Oh, K. J., Barbuto, S., Meyer, N., and Korsmeyer, S. (2004) in *The 5th Biennial Structural Biology Symposium*, Tallahassee, FL
45. Marassi, F. M., Ma, C., Gesell, J. J., and Opella, S. J. (2000) *J. Magn. Reson.* **144,** 156–161
46. Losonczi, J. A., Olejniczak, E. T., Betz, S. F., Harlan, J. E., Mack, J., and Fesik, S. W. (2000) *Biochemistry* **39,** 11024–11033
47. Boman, H. G. (1995) *Annu. Rev. Immunol.* **13,** 61–92
48. Zha, J., Weiler, S., Oh, K. J., Wei, M. C., and Korsmeyer, S. J. (2000) *Science* **290,** 1761–1765
49. Wang, J., Sykes, B. D., and Ryan, R. O. (2002) *Proc. Natl. Acad. Sci. U. S. A.* **99,** 1188–1193

ACCELERATED COMMUNICATION

Simultaneous assignment and structure determination of a membrane protein from NMR orientational restraints

FRANCESCA M. MARASSI[1] AND STANLEY J. OPELLA[2]

[1]The Burnham Institute, La Jolla, California 92037, USA
[2]Department of Chemistry and Biochemistry, University of California, San Diego, La Jolla, California 92093-0307, USA

(RECEIVED April 18, 2002; FINAL REVISION November 20, 2002; ACCEPTED November 21, 2002)

Abstract

A solid-state NMR approach for simultaneous resonance assignment and three-dimensional structure determination of a membrane protein in lipid bilayers is described. The approach is based on the scattering, hence the descriptor "shotgun," of ^{15}N-labeled amino acids throughout the protein sequence (and the resulting NMR spectra). The samples are obtained by protein expression in bacteria grown on media in which one type of amino acid is labeled and the others are not. Shotgun NMR short-circuits the laborious and time-consuming process of obtaining complete sequential assignments prior to the calculation of a protein structure from the NMR data by taking advantage of the orientational information inherent to the spectra of aligned proteins. As a result, it is possible to simultaneously assign resonances and measure orientational restraints for structure determination. A total of five two-dimensional ^{1}H/^{15}N PISEMA (polarization inversion spin exchange at the magic angle) spectra, from one uniformly and four selectively ^{15}N-labeled samples, were sufficient to determine the structure of the membrane-bound form of the 50-residue major pVIII coat protein of fd filamentous bacteriophage. Pisa (polarity index slat angle) wheels are an essential element in the process, which starts with the simultaneous assignment of resonances and the assembly of isolated polypeptide segments, and culminates in the complete three-dimensional structure of the protein with atomic resolution. The principles are also applicable to weakly aligned proteins studied by solution NMR spectroscopy.

[The structure we determined for the membrane-bound form of the Fd bacteriophage pVIII coat protein has been deposited in the Protein Data Bank as PDB file 1MZT.]

Keywords: Solid-state NMR; membrane protein; fd coat protein; protein structure determination; Pisa wheels

Solid-state NMR spectroscopy of aligned samples is a general method for determining the structures of proteins in biological supramolecular structures (Opella et al. 1987). In this article, we demonstrate that this method can be applied to membrane proteins in aligned lipid bilayers in a manner conducive to the high throughput required for structural genomics. Membrane proteins can be expressed and isotopically labeled in bacteria, isolated, purified, and reconstituted into fully hydrated lipid bilayers, which can then be aligned to a degree comparable to that observed in single crystals of small molecules (Marassi et al. 1997). "Shotgun" NMR, named for the scattered distribution of the isotopically labeled sites in the protein and the resonances in the spectra, uses the orientational information in the solid-state NMR spectra of aligned samples to simultaneously assign resonances and obtain orientational restraints for structure determination.

The alignment of samples along the direction of the applied magnetic field results in solid-state NMR spectra with resonances characterized by orientationally dependent fre-

Reprint requests to: S.J. Opella, Department of Chemistry and Biochemistry, University of California, San Diego, 9500 Gilman Drive, La Jolla, CA 92093-0307, USA; e-mail: sopella@ucsd.edu; fax: (858) 822-4821.

Article and publication are at http://www.proteinscience.org/cgi/doi/10.1110/ps.0211503.

quencies. Because nearly all residues in helical membrane proteins are immobile on the millisecond timescale of the chemical shift and heteronuclear dipole–dipole interactions, the orientational information inherent to these anisotropic nuclear spin interactions is fully manifested in high-resolution solid-state NMR spectra, and can be used for structure determination (Cross and Opella 1985; Ketchem et al. 1993; Opella et al. 1999; Wang et al. 2001). The alignment of membrane proteins in lipid bilayers is fixed by the preparation and placement of the sample in the magnetic field; therefore, each measured frequency reflects the orientation of a specific site in the protein with respect to the bilayer. Peptide plane orientations are determined directly from the NMR frequencies, and the dihedral angles ϕ and ψ, which describe the three-dimensional structure of the protein backbone, are calculated from the orientations of the peptide planes joined at the α-carbons.

The PISEMA (polarization inversion spin exchange at the magic angle) experiment (Wu et al. 1994) yields high-resolution ^{1}H–^{15}N dipolar coupling/^{15}N chemical shift separated local field spectra (Waugh 1976) of ^{15}N labeled proteins in aligned samples (Marassi et al. 1997). The orientational dependencies of these two anisotropic spin interactions serve as both the mechanisms for resolution among amide resonances, and the sources of orientational restraints for backbone structure determination. The PISEMA spectra of aligned proteins display distinctive resonance patterns that are a consequence of the direct mapping of protein structure onto NMR frequencies. These wheel-like patterns, called Pisa (polarity index slant angle) wheels, are sensitive indices of secondary structure and topology, and mirror helical wheel projections of residues in both α-helices (Marassi and Opella 2000; Wang et al. 2000) and β-strands (Marassi 2001). Similar patterns are also observed in the solution NMR spectra of weakly aligned proteins (unpublished results). The tilt (slant angle) of a helix can be determined by inspection of a Pisa wheel without resonance assignments, and only a limited amount of assignment information is needed to determine the rotation angle (polarity index) of the helix, for example, one sequential assignment or the pattern from one selectively labeled sample. This information is sufficient to characterize the architecture of a membrane protein, and also provides the starting point for the determination of the three-dimensional structure.

Previous determinations of protein structures by solid-state NMR utilized on orientational restraints derived from the frequencies of independently assigned resonances (Cross and Opella 1985; Ketchem et al. 1993; Opella et al. 1999; Wang et al. 2001). In contrast, the Shotgun NMR approach relies solely on the spectra from one uniformly, and several selectively, ^{15}N-labeled samples, and on the fundamental symmetry properties of Pisa wheels to enable the simultaneous sequential assignment of resonances and the measurement of the orientationally dependent frequencies. Crucial to Shotgun NMR is the fact that each resonance frequency in these spectra reflects molecular orientation relative to a fixed and external reference axis, defined by the direction of the applied magnetic field. This enables the structures of isolated polypeptide segments of the protein to be determined independently from each other, without propagating any associated experimental errors or uncertainties in the magnitudes and molecular orientations of the principal elements of the spin-interaction tensors. The method is demonstrated here for a highly aligned sample, using solid-state NMR experiments, but it is also applicable to weakly aligned samples using solution NMR experiments (unpublished results).

The membrane-bound form of the major pVIII coat protein of the filamentous fd bacteriophage resides within the inner membrane of infected *Escherichia coli* before incorporation into virus particles that are extruded through the cell membrane. The structure of the membrane-bound form of the protein has been extensively studied in micelle samples by solution NMR spectroscopy (Cross and Opella 1980; Henry and Sykes 1992; McDonnell et al. 1993; Van de Ven et al. 1993; Williams et al. 1996; Almeida and Opella 1997; Papavoine et al. 1998), as well as with solid-state NMR experiments on bilayer samples (Leo et al. 1987; Bogusky et al. 1988; Marassi et al. 1997). The results are in agreement in showing that the protein has two distinct α-helical segments, a short amphipathic in-plane (IP) helix that rests on the membrane surface, a longer hydrophobic transmembrane (TM) helix, and few mobile residues near the N and C termini. The same protein in intact virus particles has also been the subject of many structural studies, including solid-state NMR spectroscopy (Cross and Opella 1983, 1985; Opella et al. 1987) and X-ray fiber diffraction (Glucksman et al. 1992; Marvin et al. 1994). In this article, we describe all of the structured residues of the membrane-bound form of fd coat protein in lipid bilayers with atomic resolution.

Results

NMR spectroscopy

Structure determination begins with the acquisition of two-dimensional PISEMA spectra from one uniformly ^{15}N-labeled (Fig. 1A) and four selectively ^{15}N-labeled (Fig. 2) samples of fd coat protein in aligned lipid bilayers; the labeling patterns are illustrated at the top of Figure 1. The NMR spectra of selectively labeled samples are routinely used to assign resonances to types of amino acids in both solution NMR and solid-state NMR studies of proteins. However, in Shotgun NMR they provide much additional information, starting with the clear segregation of PISEMA spectra of helical membrane proteins into regions for the resonances from IP (lower right quadrant) and TM (upper

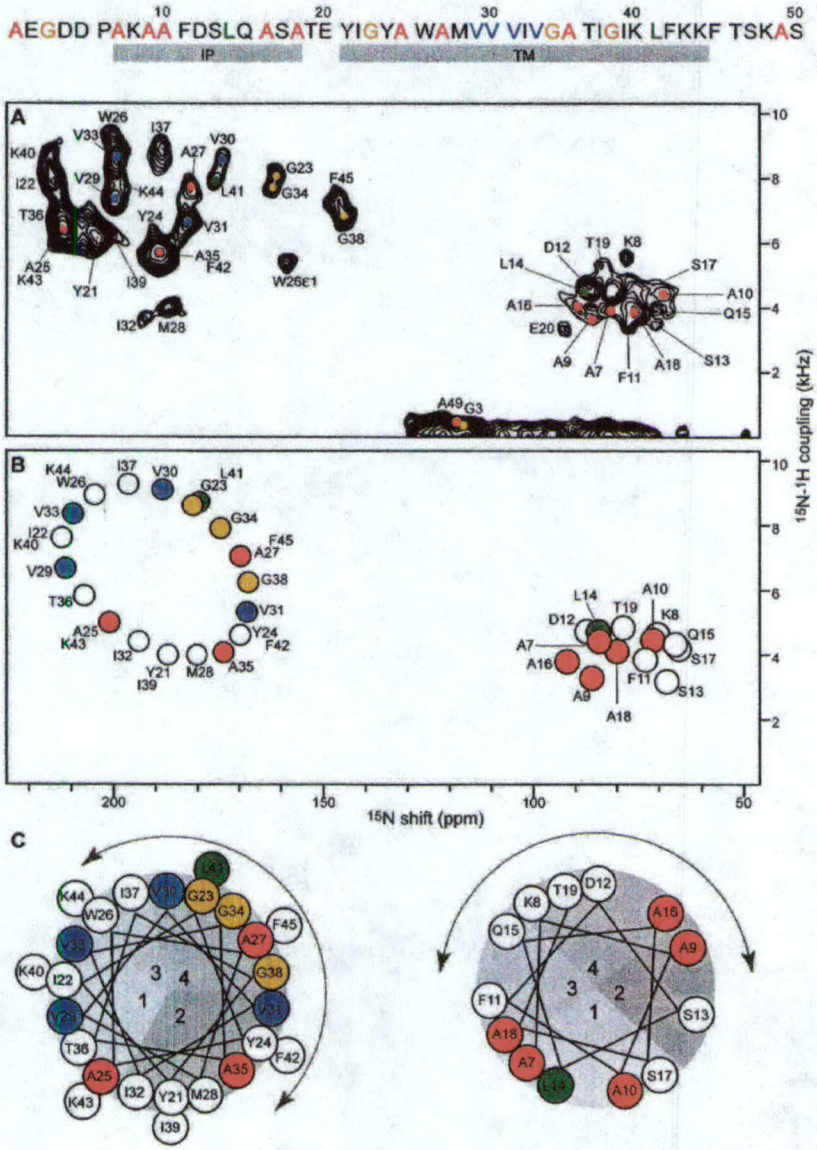

Figure 1. Two-dimensional $^{1}H/^{15}N$ PISEMA spectra of fd coat protein in aligned lipid bilayers. The amino acid sequence of the protein is shown at the top. (*A*) Experimental PISEMA spectrum obtained from uniformly ^{15}N-labeled fd coat protein in lipid bilayers. The resonance assignments are marked. (*B*) Pisa wheel PISEMA spectrum calculated from a protein model with the IP helix parallel to within 3° of the membrane surface ($\tau = 87°$), and the TM helix crossing the membrane at an angle $\tau = 30°$. The helical and Pisa wheel rotations are set to match the resonances in the experimental PISEMA spectra from the Ala (red), Gly (gold), Leu (green), and Val (blue) residues. (*C*) Helical wheel representations of the protein IP and TM helices. The curved arrows span the N-terminal periplasmic side of the membrane.

left quadrant) residues. For example, of the 10 resonances observed in the spectrum of ^{15}N-Ala-labeled coat protein, five are in the IP region of the spectrum, including that from Ala 18, which establishes that the IP helix extends at least to residue 18 (Fig. 2A); three resonances are in the TM region; one is isotropic because of motional averaging, which demonstrates that Ala 49 next to the C terminus is mobile on the millisecond timescale; and the N-terminal Ala 1 gives a peak at 35 ppm (not shown in these spectra). Of the four Gly resonances (Fig. 2B), three are in the TM region, and one, assigned to Gly 3 (Bogusky et al. 1987), is from a residue near the mobile N terminus. The chemical shift frequencies of the Gly resonances are upfield of the others, as expected based on the differences in the magni-

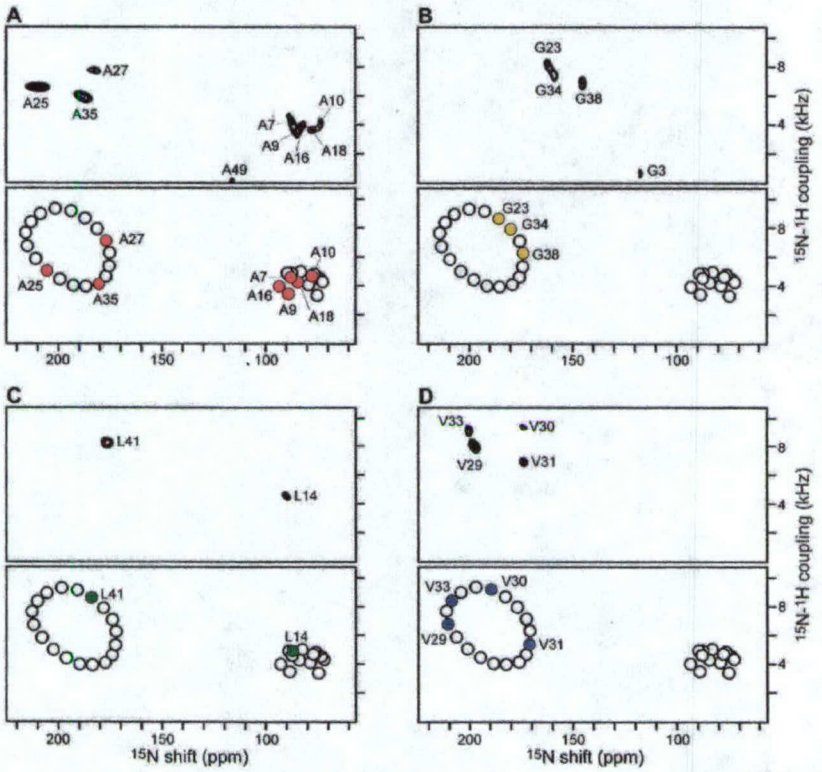

Figure 2. Experimental and calculated $^{1}H/^{15}N$ PISEMA spectra for the TM region of the fd coat protein, in aligned lipid bilayers selectively ^{15}N-labeled with (*A*) Ala, (*B*) Gly, (*C*) Leu, and (*D*) Val. The resonances were assigned to specific amino acids in the sequence by comparison of the experimental spectrum (*top*) with the Pisa wheel spectrum (*bottom*). In each panel, the Pisa wheel PISEMA spectrum was calculated from a protein model with the IP helix tilted by $\tau = 87°$, and the TM tilted by $\tau = 30°$.

tudes of the principal values of the amide ^{15}N chemical shift tensors for this amino acid (Oas et al. 1987). The two Leu resonances in the spectrum in Figure 2C are straightforwardly assigned to Leu 14 in the IP region and Leu 41 in the TM region (Marassi et al. 1997). As expected, the resonances from the four valine residues in the protein are in the TM region of the spectrum (Fig. 2D).

The observation of Pisa wheels in both the IP and TM regions of the spectrum of the uniformly ^{15}N-labled sample (Fig. 1A), by itself, leads to an initial trial model of the protein with two α-helices, one crossing the membrane with a tilt angle (τ) of 30°, the other resting within 3° of parallel to the membrane surface ($\tau = 87°$). This model is sufficient for the calculation of the idealized PISEMA spectrum shown in Figure 1B. Each helix in the trial model is separately rotated around its axis until the resonance pattern in its calculated Pisa wheel spectrum qualitatively matches the resonances in the experimental spectra of selectively labeled samples. This is illustrated with the helical wheel projections of the two helices in Figure 1C, and with the four Pisa wheel spectra in Figure 2. This procedure yields both the rotation of the two helices about their long axes (ρ), as well as the sequential assignments of the resonances observed in the experimental spectra. Up to this stage, starting with no independently assigned resonances, the procedure has determined the tilt and rotation of both helices with high precision, the lengths of both helices within a few residues, the backbone dynamics qualitatively, and the sequential assignments of resonances from 19 out of the 48 amide backbone sites in the protein.

In the second step, the ^{15}N chemical shift and ^{1}H–^{15}N dipolar coupling frequencies are measured for each resonance in the experimental PISEMA spectrum of the uniformly ^{15}N-labeled sample, and used to calculate the orientations of their corresponding peptide planes. These frequencies provide the restraints for three-dimensional structure determination, because they depend on the orientation of the corresponding molecular site with respect to the direction of the applied magnetic field, and on the magnitudes and orientations of the principal elements of the spin-interaction tensors at that site. The ^{15}N chemical shift frequency is given by:

$$\nu_{N\ shift} = \sigma_{11} \sin^2(\alpha - \delta) \sin^2\beta + \sigma_{22} \cos^2\beta + \sigma_{33} \cos^2(\alpha - \delta) \sin^2\beta \quad (1)$$

where σ_{11}, σ_{22}, and σ_{33} are the principal elements of the ^{15}N chemical shift tensor, and δ is the angle between σ_{33} and the NH bond. The ^{1}H–^{15}N dipolar coupling frequency is given by:

$$\nu_{NH\ cplg} = \gamma_H\gamma_N h/r^3 (3 \sin^2\beta \cos^2 \alpha - 1) \quad (2)$$

where γ_H and γ_N are the gyromagnetic ratios of the nuclei, h is Planck's constant, and r is the NH bond length. In both equations, α and β are the polar angles that describe the peptide plane orientation in the magnetic field: α is the angle between the NH bond and the projection of the magnetic field direction on the peptide plane, and β is the angle between the normal to the peptide plane and the direction of the magnetic field (Tycko et al. 1986; Opella et al. 1987). The amide ^{15}N chemical shift tensor and the NH bond length are well characterized in model peptides (Oas et al. 1987; Wu et al. 1995), and can be used to extract α/β orientational restraints from the resonance frequencies using Equations 1 and 2.

The symmetry properties of the spin-interaction tensors give rise to degeneracies in the angular restraints. Each equation yields combinations of the angles α and β that are consistent with a frequency measurement, and that trace out a line on the α/β surface. The actual orientation of a peptide plane must satisfy both Equations 1 and 2 and corresponds to a single α/β point. The orientation is determined for $0 < \alpha < 180$ and $0 < \beta < 90$, so that any one of the four orientations (α/β), $(\alpha/180 - \beta)$, $(180 + \alpha/\beta)$, and $(180 + \alpha/180 - \beta)$ are consistent with the experimental data. In addition, because the signs of the ^{1}H–^{15}N dipolar couplings are not determined in these experiments, resonances with couplings smaller than the half-maximal value (~5 kHz as displayed) can have two possible α/β solutions, resulting in up to eight symmetry-related peptide plane orientations; however, because the dipolar couplings for TM helices with tilt angles <40° are positive, and those for IP helices are negative, the set of restraints is reduced to four symmetry-related orientations for each plane in the initial structural model.

The next step involves the calculation of the ϕ and ψ dihedral angles from the α/β orientational restraints of pairs of connected peptide planes (Opella et al. 1987; Quine and Cross 2000; Opella et al. 2001). Because at this stage of the analysis only the selectively labeled resonances are definitively assigned, we first perform this calculation for all combinations of α/β restraint sets, where for n resonances, there are a total of $(n^2 - n)$ sets of ϕ/ψ. Each dipeptide combination has two pairs of dihedral angles, each of which satisfies the requirement for tetrahedral geometry and L-amino acid chirality at the α-carbon, and because each peptide plane has four possible orientations, this results in 32 possible ϕ/ψ sets. However, only 16 of these are unique, because we do not differentiate between positive and negative magnetic field directions. Typically, only one of these is energetically favorable and can be identified using a Ramachandran map.

Orientational ambiguities can also be resolved using additional properties of Pisa wheels (Marassi and Opella 2002). In an α-helix, the orientation of each peptide plane can be predicted from the angles τ and ρ, so that it is possible to select a single orientation, out of the symmetry-related set of four, from its resonance position in the NMR Pisa wheel (Marassi and Opella 2002). This is illustrated in Figure 1C, in which the pie-shaped sections labeled 1, 2, 3, and 4 in the helical wheels (Pisa pies), correspond, respectively, to the four orientations 1 (α/β), 2 $(\alpha/180 - \beta)$, 3 $(180 + \alpha/\beta)$, and 4 $(180 + \alpha/180 - \beta)$. For example, the Val 29 peptide plane has an orientation defined by 1 (α/β). It is connected to the Val 30 peptide plane with orientation 4 $(180 + \alpha/180 - \beta)$, which, in turn, connects to Val 31 with orientation 2 $(\alpha/180 - \beta)$. It is the ability to resolve the orientational ambiguities that enables the sequential assignment of the remaining resonances in the spectrum of the uniformly ^{15}N-labeled protein, including those that are not represented in spectra of selectively ^{15}N-labeled samples.

The chemical shift and dipolar coupling frequencies of the PISEMA resonances provide the input for protein structure determination. We begin by constructing isolated segments of structure for the assigned resonances in the sequences: Ala 9–Ala 10, Val 29–Val 30–Val 31, and Val 33–Gly 34. These segments constitute the starting point in a search for the peptide planes and associated resonances that link them. For example, a single residue, Ile 32, whose resonance is unassigned at this stage, separates the peptide segments Val 29–Val 30–Val 31 and Val 33–Gly 34. Because the resonance of Ile 32 falls in section 2 of the helical wheel (Fig. 1C), its peptide plane must have an orientation defined by 2 $(\alpha/180 - \beta)$, and it must have helical dihedral angles to its neighboring peptide planes. The Ile 32 resonance is assigned by searching the entire set of calculated dihedral angles for a peptide plane combination that satisfies these conditions. The resonances for Met 28 linking the assigned Ala 27 to the Val 29 segment and for Trp 26 linking the assigned Ala 25 and Ala 27 are obtained in a similar fashion. The search is performed for all unlinked planes and segments of planes, until all resonances have been assigned, including those of the turn connecting the two helices, and the indole nitrogen of Trp 26 (Ramamoorthy et al. 1997). Because resonance assignment is accompanied by determination of the calculated restraints and dihedral angles, the structure of the protein is determined.

Structure of a membrane protein in lipid bilayers

The three-dimensional structure of the membrane-bound form of fd coat protein in lipid bilayers is shown in Figure

3. The 16-Å-long IP helix (residues 8–18) is amphipathic and rests on the membrane surface, with the boundary separating the polar and apolar residues parallel to the lipid bilayer surface, and the apolar residues facing the hydrocarbon core of the lipid bilayer (Fig. 3C). The aromatic residues, Phe 11 in the IP helix, and Tyr 21 in the TM helix, are near this boundary region, and approximately equidistant from the hydrophobic central core of the lipid bilayers (Fig. 3A).

The 35-Å-long TM helix (residues 21–45) crosses the membrane at an angle of 26° up to residue Lys 40, where the helix tilt changes to 16°. A similar change in helix direction at this site was also observed in the structure of the protein in the phage particles determined by solid-state NMR spectroscopy (Cross and Opella 1985). The helix tilt accommodates the thickness of the phospholipid bilayer, which is ~31 Å for the lipids, palmitoyl-oleoyl-phosphatidylcholine and -phosphatidylglycerol, used in this study, and typical of *E. coli* membrane components. Tyr 21 and Phe 45 at the lipid–water interfaces delimit the TM helix. The Trp 26 side chain intercalates in the hydrophobic bilayer interior (Fig. 3A) with an orientation relative to the hydrophobic helix similar to that found for the coat protein in bacteriophage particles (Cross and Opella 1983). The indole NH bond points toward the N terminus and into the lipid–water interface, where it can hydrogen-bond with either water or the phospholipid head groups. Interfacial indole side chains oriented in this way are likely to play a role in determining membrane protein orientation (Schiffer et al. 1992). The TM helix is rotated so that the charged residues, Lys 40, Lys 43, and Lys 44, and the polar residue Thr 36, face the C-terminal, cytoplasmic side of the protein (Fig. 3A). This topology may have functional significance for the bacteriophage assembly process, during which the cytoplasmic, single-stranded, phage DNA is extruded through the inner bacterial membrane after being enclosed within a tube of coat protein subunits. The TM helix orientation is such that it enables the charged amino groups of the lysine side chains to emerge from the membrane interior, and become available at the membrane surface for DNA binding during bacteriophage extrusion.

The TM and IP helices are connected by a short turn (Thr 19–Glu 20) that differs from the longer loop (residues 17–26) determined for the same protein in lipid micelles (Almeida and Opella 1997). This may be due to differences between the micelle and bilayer environments, or to the limitations with working with the few long-range NOE restraints observed in solution NMR studies of helical membrane proteins. Both reasons strongly support an argument in favor of the use of lipid bilayer samples for structure determination of membrane proteins. For the structure determination of the turn between the two helices, the 16 sets of calculated ϕ/ψ dihedral angles were reduced to 8 for both Thr 19 and Glu 20, because of the restraints imposed by the peptide plane orientations of the flanking amino acid residues, Ala 18 and Tyr 21, and linking the Thr 19 and Glu 20 peptide planes resulted in 16 possible conformations for the turn. Although the tilt and rotation of the IP and TM helices are determined independently of the connecting turn, their relative orientations are defined by the turn geometry, and are different for each turn conformation. The resulting structures can be grouped into four families (Fig. 4A–D), each with a similar (within 10°) relative orientation of the IP and TM helices. Ten conformations including one conformation

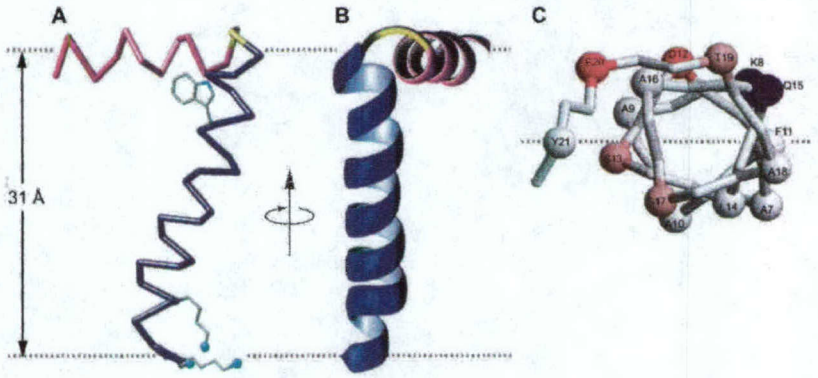

Figure 3. Structure of the membrane-bound form of fd coat protein in lipid bilayers, with the IP helix in magenta, the TM helix in blue, and the short connecting turn in yellow. The flexible N and C termini are not shown. The dashed gray lines mark the lipid–water boundary. (*A*) Side view showing the 26° tilt of the TM helix. The Trp 26 side chain is shown in its experimentally determined orientation. The direction of the applied magnetic field is parallel to the arrow. The Lys 40, Lys 43, and Lys 44 side chains were modeled in MolMol and face the cytoplasmic side of the membrane. (*B*) Front view. (*C*) View of the IP helix down from the C terminus. The α-carbons are shown as spheres. The dashed gray line representing the membrane–water interface also marks the boundary between hydrophilic (colored) and hydrophobic (gray) residues. The coordinates have been deposited to the Protein Data Bank (PDB file 1MZT).

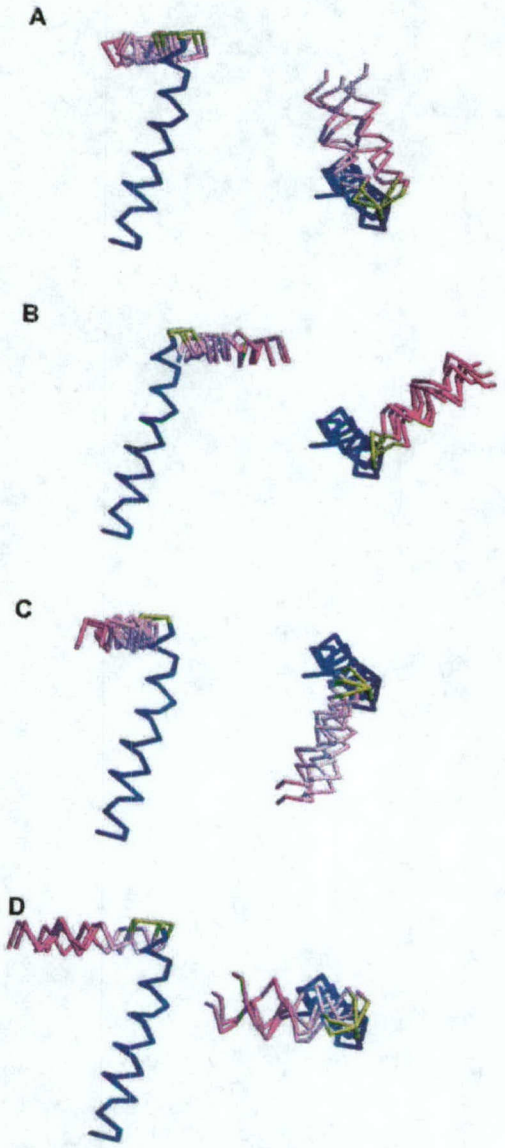

Figure 4. Side and top views of the four structural families obtained for the 16 different geometries of the connecting turn (yellow). Each family (A–D) contains four structures in which the relative orientations of the IP (magenta) and TM (blue) helices are similar and defined by the turn geometry. Family A (*A*) contains the structure with the most favorable connecting turn geometry (Thr 19 ϕ/ψ = –93/–82; Glu 20 ϕ/ψ = –37/132; PDB file 1MZT). Family B (*B*), family C (*C*), and family D (*D*) contain structures with unfavorable connecting turn geometries.

in family A, one in family B, and all conformations in family C and family D, could be discarded because they have steric clashes between the IP and TM helices. The six remaining structures belong to family A or B (Fig. 4A,B), and only one structure in family A has the most favorable geometry at the connecting turn, and it has been deposited in the Protein Data Bank (PDB file 1MZT), whereas the other structures have less realistic values for the backbone dihedral angles ϕ/ψ, that map in forbidden regions of the Ramachandran map. The resulting structure, shown in Figure 3, is particularly appealing because the dihedral angles of the connecting turn do not disrupt the sense of helix winding as the protein structure makes the transition from the N-terminal IP helix to the C-terminal TM helix. This is suggestive of a helix-wind-up conformational change during the phage assembly process, whereby tightening the winding around the connecting turn forces the IP helix to tilt up and to form the single, continuous, long α-helix observed in the phage-bound protein structure (Opella et al. 1987; Glucksman et al. 1992; Marvin et al. 1994). This is also consistent with the model for bacteriophage assembly proposed by Papavoine et al. (1998).

Discussion

The ability to calculate a backbone structure solely from the orientationally dependent ^{15}N chemical shift and ^{1}H–^{15}N dipolar coupling frequencies measured in PISEMA spectra of uniformly and selectively ^{15}N-labeled proteins paves the way for rapid automated methods of protein structure determination. In the Shotgun NMR approach to structure determination, a structural model of the protein is first generated by pattern recognition of the resonances in the PISEMA spectrum of a uniformly ^{15}N-labeled sample, which is then used to calculate an idealized spectrum and model of the protein. The data from a few selectively ^{15}N-labeled samples enable the tilt and rotation of the helices to be determined, and in a more detailed analysis to simultaneously assign all of the resonances and calculate the three-dimensional structure of the protein. Thus, for the fd coat protein, whereas the initial structural model is determined solely from Pisa wheels and consists of two ideal α-helices, the final structure resolves a distinct kink near residue 39, which changes the direction of the TM helix. The quality of the structure cannot be described in terms of a conventional RMSD, because a unique structure is determined from the experimental data. For comparison, the ability to identify subtle structural features, such as a kink in an otherwise uniform helix, can be accomplished in structures determined by X-ray crystallography only when the resolution is 2Å or better. Thus, the structures determined by solid-state NMR of aligned samples have an effective resolution that rivals that of the best experimental determinations of proteins by other methods.

There are two classes of membrane proteins with structures dominated by α-helices or β-strands. Although the class of protein is generally known, before structure determination is initiated, from sequence analysis or other spectroscopic methods, solid-state NMR of aligned samples is also able to distinguish between these two cases. The Shotgun NMR approach, as described here, relies on being able

to detect Pisa wheel patterns of resonances that reflect the protein structure in the spectra of oriented proteins. In the case of fd coat protein, the spectra reflect helical structure; however, regular Pisa wheel patterns are also predicted for β-strands (Marassi 2001), so there is every reason to believe that the Shotgun NMR approach will be equally applicable to this class of proteins. The structure determinations of the turns and loops are, in principle, more complex, but enormous simplifications result from the structural constraints imposed by the flanking secondary-structure elements. For example, in the case of fd coat protein, the tilts and rotations of the two helices place strong steric restraints on the allowed conformations of residues in the turn connecting the two helices, thus limiting the result to a single structure of the backbone. The structures of nitrogen-containing side chains are also readily determined, and extensions of the approach to ^{13}C will enable the structures of all side chains to be included.

The Shotgun NMR approach for simultaneously assigning spectra and determining structures by solid-state NMR of aligned samples is generally applicable. A total of five two-dimensional PISEMA spectra were sufficient for structure determination of this 50-residue protein. Simulations and unpublished experimental results indicate that this approach can be applied directly to proteins two to three times larger and, with the use of higher dimensional experiments and stronger magnetic fields, to substantially larger proteins. Aligned bilayer samples can be prepared from proteins that are expressed and labeled in bacteria or other systems, only a few experimental spectra are required, and data analysis methods can be automated. Therefore, this method has the potential for high-throughput structure determination of membrane proteins.

Materials and methods

The preparation of samples of ^{15}N-labeled fd coat protein in aligned lipid bilayers and the details of NMR experiments have been described (Marassi et al. 1997). NMR spectra were obtained on a Chemagnetics-Otsuka Electronics spectrometer with a wide bore Oxford 400/89 magnet, using a home-built flat-coil probe double-tuned to the resonance frequencies of ^{1}H at 400.4 MHz, and ^{15}N at 40.6 MHz. The structure calculations were performed using a suite of Fortran programs developed in our laboratories. Peptide plane orientations were calculated from the input NMR frequencies and the values of the spin-interaction tensors, in terms of α/β polar angles, using Equations 1 and 2 in the program RESTRICT. Dihedral angles were calculated by constraining tetrahedral geometry around the common α-carbon of adjoining peptide planes, of known orientation (Opella et al. 1987, 1999; Quine and Cross 2000) using the program ABtoTOR. The program uses standard peptide plane geometry and the dihedral angle $\omega = 180°$. The principal values and molecular orientation of the amide ^{15}N chemical shift tensor were $\sigma_{11} = 64$ ppm; $\sigma_{22} = 77$ ppm; $\sigma_{33} = 217$ ppm; $\delta = 17°$, and the NH bond distance was 1.07 Å (Wu et al. 1995). The values and orientation of the amide ^{15}N chemical shift tensor for Gly residues were $\sigma_{11} = 41$ ppm; $\sigma_{22} = 64$ ppm; $\sigma_{33} = 210$ ppm; and $\delta = 18°$ (Oas et al. 1987). PDB coordinates were calculated, from the resulting protein structure and orientation in the lipid bilayers, using the programs TORtoPDB and ROTPDB. Calculation of spectra from structural coordinates was performed using the program PDBtoNMR. The structure was rendered using MolMol (Koradi et al. 1996) and RasMol (Sayle and Milner-White 1995). The coordinates have been deposited in the Protein Data Bank (PDB file 1MZT).

The orientation of the Trp 26 indole side chain was obtained using Equations 1 and 2, in which α was redefined as the angle between the indole NH bond and the projection of the magnetic field direction on the aromatic plane, and β as the angle between the normal to the aromatic indole plane and the direction of the magnetic field. The values and orientation of the indole $^{15}N_{\varepsilon 1}$ chemical shift tensor were $\sigma_{11} = 61$ ppm; $\sigma_{22} = 130$ ppm; $\sigma_{33} = 181$ ppm; $\delta = 0°$, and the NH bond distance was 1.07 Å (Ramamoorthy et al. 1997). Of the four possible symmetry-related orientations, two lead to atomic overlap. The remaining two orientations each have the indole NH bond pointing toward the protein N terminus or away from it. We chose the first because it places the NH bond at the lipid–water interface, and enables hydrogen-bonding with water.

Acknowledgments

This research was supported by grants R37GM24266, RO1CA82864, RO1GM29754, and PO1GM56538 from the National Institutes of Health, and grants DAMD17-00-1-0506 and DAMD17-02-1-0313 from the Department of the Army. It used the Resource for Solid-State NMR of Proteins, supported by grant P41RR09731, from the Biomedical Research Technology Program, National Center for Research Resources, National Institutes of Health.

The publication costs of this article were defrayed in part by payment of page charges. This article must therefore be hereby marked "advertisement" in accordance with 18 USC section 1734 solely to indicate this fact.

References

Almeida, F.C. and Opella, S.J. 1997. fd coat protein structure in membrane environments: Structural dynamics of the loop between the hydrophobic trans-membrane helix and the amphipathic in-plane helix. *J. Mol. Biol.* **270:** 481–495.

Bogusky, M.J., Schiksnis, R.A., Leo, G.C., and Opella, S.J. 1987. Protein backbone dynamics by solid state and solution ^{15}N NMR spectroscopy. *J. Magn. Reson.* **72:** 186–190.

Bogusky, M.J., Leo, G.C., and Opella, S.J. 1988. Comparison of the dynamics of the membrane bound form of fd coat protein in micelles and in bilayers. *Proteins: Struct. Funct. Genetics* **4:** 123–130.

Cross, T.A. and Opella, S.J. 1980. Structural properties of fd coat protein in sodium dodecyl sulfate micelles. *Biochem. Biophys. Res. Commun.* **92:** 478–484.

———. 1983. Protein structure by solid-state NMR. *J. Am. Chem. Soc.* **105:** 306–308.

———. 1985. Protein structure by solid-state NMR: Residues 40–45 of bacteriophage fd coat protein. *J. Mol. Biol.* **182:** 367–381.

Glucksman, M.J., Bhattacharjee, S., and Makowski, L. 1992. Three-dimensional structure of a cloning vector: X-ray diffraction studies of filamentous bacteriophage M13 at 7 Å resolution. *J. Mol. Biol.* **226:** 455–470.

Henry, G.D. and Sykes, B.D. 1992. Assignment of amide ^{1}H and ^{15}N NMR resonances in detergent-solubilized M13 coat protein: A model for the coat protein dimer. *Biochemistry* **31:** 5284.

Ketchem, R.R., Hu, W., and Cross, T.A. 1993. High-resolution conformation of gramicidin A in a lipid bilayer by solid-state NMR. *Science* **261:** 1457–1460.

Koradi, R., Billeter, M., and Wüthrich, K. 1996. MOLMOL: A program for

display and analysis of macromolecular structures. *J. Mol. Graphics* **14:** 51–55.

Leo, G.C., Colnago, L.A., Valentine, K.G., and Opella, S.J. 1987. Dynamics of fd coat protein in lipid bilayers. *Biochemistry* **26:** 854–862.

Marassi, F.M. 2001. A simple approach to membrane protein secondary structure and topology based on NMR spectroscopy. *Biophys. J.* **80:** 994–1003.

Marassi, F.M. and Opella, S.J. 2000. A solid-state NMR index of membrane protein helical structure and topology. *J. Magn. Reson.* **144:** 150–155.

———. 2002. Using Pisa pies to resolve ambiguities in angular constraints from PISEMA spectra of aligned proteins. *J. Biomol. NMR* **23:** 239–242.

Marassi, F.M., Ramamoorthy, A., and Opella, S.J. 1997. Complete resolution of the solid-state NMR spectrum of a uniformly ^{15}N-labeled membrane protein in phospholipid bilayers. *Proc. Natl. Acad. Sci.* **94:** 8551–8556.

Marvin, D.A., Hale, R.D., Nave, C., and Citterich, M.A. 1994. Molecular models and structural comparisons of native and mutant class I filamentous bacteriophages Ff (fd, f1, MI3), Ifl and Ike. *J. Mol. Biol.* **235:** 260–286.

McDonnell, P.A., Shon, K., Kim, Y., and Opella, S.J. 1993. fd coat protein structure in membrane environments. *J. Mol. Biol.* **233:** 447–463.

Mesleh, M.F., Veglia, G., DeSilva, T.M., Marassi, F.M., and Opella, S.J., 2002. Dipolar waves as NMR maps of protein structure. *J. Am. Chem. Soc.* **124:** 4206–4207.

Oas, T.G., Hartzell, C.J., Dahlquist, W., and Drobny, G.P. 1987. The amide ^{15}N chemical shift tensors of four peptides determined from ^{13}C dipole-coupled chemical shift powder patterns. *J. Am. Chem. Soc.* **109:** 5962–5966.

Opella, S.J., Stewart, P.L., and Valentine, K.G. 1987. Protein structure by solid-state NMR Spectroscopy. *Q. Rev. Biophys.* **19:** 7–49.

Opella, S.J., Marassi, F.M., Gesell, J.J., Valente, A.P., Kim, Y., Oblatt-Montal, M., and Montal, M. 1999. Structures of the M2 channel-lining segments from nicotinic acetylcholine and NMDA receptors by NMR spectroscopy. *Nat. Struct. Biol.* **6:** 374–379.

Opella, S.J., Ma, C., and Marassi, F.M. 2001. NMR of membrane associated peptides and proteins. *Methods Enzymol.* **339:** 285–313.

Papavoine, C.H.M., Christiaans, B.E.C., Folmer, R.H.A., Konings, R.N.H., and Hilbers, C.W. 1998. Solution structure of the M13 major coat protein in detergent micelles: A basis for a model of phage assembly involving specific residues. *J. Mol. Biol.* **282:** 401–419.

Quine, J.R. and Cross, T.A. 2000. Transmembrane protein structure from NMR. *Concepts Magn. Reson.* **12:** 71.

Ramamoorthy, A., Wu, C.H., and Opella, S.J. 1997. Magnitudes and orientations of the principal elements of the ^{1}H chemical shift, ^{1}H–^{15}N dipolar coupling, and ^{15}N chemical shift interaction tensors in ^{15}N-tryptophan and ^{15}N-histidine side chains determined by three-dimensional solid-state NMR spectroscopy. *J. Am. Chem. Soc.* **119:** 10479–10486.

Sayle, R. and Milner-White, E.J. 1995. RASMOL: Biomolecular graphics for all. *Trends Biochem. Sci.* **20:** 374–376.

Schiffer, M., Chang, C.H., and Stevens, F.J. 1992. The functions of tryptophan residues in membrane proteins. *Protein Eng.* **5:** 213–214.

Tycko, R., Stewart, P.L., and Opella, S.J. 1986. Peptide plane orientations determination by fundamental and overtone nitrogen 14 NMR. *J. Am. Chem. Soc.* **108:** 5419–5425.

Van de Ven, F.J.M., Os, J.W.M., Aelen, J.M.A., Wymenja, S.S., Remerowski, M.L., Konings, C.W., and Hilbers, R.N.H. 1993. Assignment of ^{1}H and backbone ^{13}C resonances in detergent-solubilized M13 coat protein via multinuclear multidimensional NMR: A model for the coat protein monomer. *Biochemistry* **32:** 8322.

Wang, J., Denny, J., Tian, C., Kim, S., Mo, Y., Kovacs, F., Song, Z., Nishimura, K., Gan, Z., Fu, R., et al. 2000. Imaging membrane protein helical wheels. *J. Magn. Reson.* **144:** 162–167.

Wang, J., Kim, S., Kovacs, F., and Cross, T.A. 2001. Structure of the transmembrane region of the M2 protein H^{+} channel. *Protein Sci.* **10:** 2241.

Waugh, J.S. 1976. Uncoupling of local field spectra in nuclear magnetic resonance: Determination of atomic positions in solids. *Proc. Natl. Acad. Sci.* **73:** 1394.

Williams, K.A., Farrow, N.A., Deber, C.M., and Kay, L.E. 1996. Structure and dynamics of bacteriophage IKe major coat protein in MPG micelles by solution NMR. *Biochemistry* **35:** 5145–5157.

Wu, C., Ramamoorthy, A., and Opella, S.J. 1994. High-resolution heteronuclear dipolar solid-state NMR spectroscopy. *J. Magn. Reson. A* **109:** 270–272.

Wu, C., Ramamoorthy, A., Gierasch, L.M., and Opella, S.J. 1995. Simultaneous characterization of the amide ^{1}H chemical shift, ^{1}H–^{15}N dipolar, and ^{15}N chemical shift interaction tensors in a peptide bond by three-dimensional solid-state NMR spectroscopy. *J. Am. Chem. Soc.* **117:** 6148–6149.